



Molecular-level understanding of metal ion retention in clay-rich materials

Xiandong Liu, Christophe Tournassat, Sylvain Grangeon, Andrey Kalinichev, Yoshio Takahashi, Maria Marques Fernandes

► To cite this version:

Xiandong Liu, Christophe Tournassat, Sylvain Grangeon, Andrey Kalinichev, Yoshio Takahashi, et al.. Molecular-level understanding of metal ion retention in clay-rich materials. *Nature Reviews Earth & Environment*, 2022, 3, pp.461-476. 10.1038/s43017-022-00301-z . insu-03714436

HAL Id: insu-03714436

<https://insu.hal.science/insu-03714436>

Submitted on 26 Jan 2023

HAL is a multi-disciplinary open access archive for the deposit and dissemination of scientific research documents, whether they are published or not. The documents may come from teaching and research institutions in France or abroad, or from public or private research centers.

L'archive ouverte pluridisciplinaire **HAL**, est destinée au dépôt et à la diffusion de documents scientifiques de niveau recherche, publiés ou non, émanant des établissements d'enseignement et de recherche français ou étrangers, des laboratoires publics ou privés.

Molecular-level understanding of metal ion retention in clay-rich materials

Xiandong Liu^{1†}, Christophe Tournassat^{2,3†}, Sylvain Grangeon⁴, Andrey G. Kalinichev⁵,
Yoshio Takahashi⁶, Maria Marques Fernandes⁷

1. State Key Laboratory for Mineral Deposits Research and School of Earth Sciences and Engineering,
Nanjing University, Nanjing, China

2. Institut des Sciences de la Terre d'Orléans, Université d'Orléans–CNRS–BRGM, Orléans, France

3. Earth and Environmental Sciences Area, Lawrence Berkeley National Laboratory, Berkeley, CA, USA

4. BRGM, Orléans, France

5. Laboratoire de physique subatomique et technologies associées , École nationale supérieure Mines-
Télécom Atlantique Bretagne Pays de la Loire , Nantes, France

6. Department of Earth and Planetary Science, The University of Tokyo, Tokyo, Japan

7. Laboratory for Waste Management, Paul Scherrer Institute, Villigen, Switzerland

† Corresponding author: xiandongliu@nju.edu.cn; christophe.tournassat@univ-orleans.fr.

Abstract

Clay minerals retain or adsorb metal ions in the Earth's critical zone. Rocks, sediments and soils rich in clay minerals can concentrate rare earth elements (REEs) in ion-adsorption type deposits and are similarly effective at metallic contaminant remediation. However, the molecular-scale chemical and physical mechanisms of metal retention remain only partly understood. In this Review, we describe the nature, location and energy requirements of metal retention at clay mineral surfaces. Retention originates mainly from electrostatic interactions during cation exchange at low pH and chemical bonding in surface complexation and precipitation at neutral and high pH. Surface complexation induces surface redox reactions and precipitation mechanisms including neoformation of clay minerals layered structure. In ion-adsorption type deposits, outer-sphere adsorption is the major retention mechanism of REE ions. By contrast, the use of clay minerals in pollution control relies on various mechanisms that can coexist, including cation exchange, surface complexation and nucleation-growth. To more effectively leverage clay mineral-metal interactions in resource recovery and contaminant remediation, complex mechanisms such as surface precipitation and redox reactions must be better understood; for instance, by utilizing advances in quantum mechanical calculations, close combination between synchrotron and simulation techniques, and upscaling of molecular-level information in macroscopic thermokinetic predictive models.

[H1] Introduction

Clay minerals [G] play a major role in scavenging metal ions [G]¹ in Earth's critical zone [G]. Metal immobilization processes are key aspects of natural biogeochemical cycles in surficial environments, as clay minerals can control the bioavailability of metal nutrients K^+ and Ca^{2+} in temperate-zone soils². In addition, the adsorptive properties of clay-rich materials [G] make them of economic interest, as they are crucial to concentrating rare earth elements (REEs) from weathered granites onto clay surfaces during the formation of ion-adsorption type deposits³. Clay-rich materials are also of growing industrial interest owing to their effective metal retention capacity and their cheap, widespread availability. For example, clay minerals are commonly used in pollution control and remediation applications, including as containment barriers in radioactive waste repository concepts⁴, as liner materials in landfills⁵, or as remediation agents for heavy metal-polluted soils⁶. The interaction of clay minerals and metal ions is therefore critical to environmental, industrial and economic applications. However, the complex and diverse nature of clay minerals and their surfaces mean that the mechanisms of metal retention remain debated.

The distinctive interaction of clay minerals with metal ions stems from their surface properties, which result from their layered crystal structure (Box 1 and Figure 1)⁷. Individual clay layers are formed of an octahedral sheet [G] sandwiched between two tetrahedral sheets [G], often

called **2:1 layers** [G] (Figure 1). When stacked together, these layers create inner, outer and edge surfaces onto which metal ions can be adsorbed. However, each layer can have varying compositions, meaning OH groups and cation exchange sites have a range of surface positions (Box 1). Various OH groups exist (such as those coordinated to Si, Al, Mg, Fe) and they are responsible for the chemical bonding of metal ions. This variety of surface positions, surface groups and layer compositions lead to a diversity of retention processes, such as cation exchange, surface complexation, structural incorporation in clay layers or through mineral growth by **epitaxial nucleation** [G]⁸.

Bulk measurements of metal retention in batch experiments do not always provide enough information to predict the fate of metal ions in practical or real-life applications in clay-rich media. Extrapolating the results of batch adsorption experiments (with timescales from hours to days) directly to radionuclide retention predictions in radioactive waste disposal in a geological formation (with timescales over hundreds and thousands of years) can lead to erroneous conclusions because the various retention processes do not have the same kinetic and reversibility characteristics. Consequently, molecular-level knowledge is crucial for understanding the physical-chemical mechanisms underlying experimental and field observations, and for developing predictive models for these environments^{6,9}.

The emergence of several experimental techniques (such as **neutron diffraction**¹⁰ [G], **synchrotron X-ray reflectivity (XRR)**¹¹ [G] and **X-ray absorption spectroscopy (XAS)** [G]^{12,13}) in the late 1980s, accompanied by the rapid development of computational modelling approaches (quantum mechanical, classical and multiscale)¹⁴, has provided the necessary tools for exploring clay mineral-metal ion interactions over different time scales. Because of the high surface heterogeneity of clay minerals, some of the basic properties controlling metal ion retention can be quantified only with the combination of advanced experimental and molecular simulation methods. Multiscale simulation methods in particular are a powerful tool for providing parameters that are impossible or very difficult for experiments to achieve, such as predicting the behavior of metal ions in clay-rich media over geological timescales¹⁵.

In this Review, we discuss advances in understanding metal ion-clay mineral interactions at the molecular scale. We first explore the macroscopic factors that affect the adsorptive properties of clay minerals, such as the composition and pH of the aqueous solution. Next, immobilization processes are described separately for basal and edge surfaces because they have fundamental differences in bonding mechanisms of with metal ions. We then review the importance of metal retention processes in ion adsorption REE ore formation and pollution control engineering, and we highlight possible future research directions in the molecular-level view of clay mineral-metal ion interactions for fundamental and applied research.

[H1] Macroscopic environmental factors

Under favourable conditions, 1 kg of smectite [G] such as montmorillonite can sorb up to 100 g of metal cations, or equivalently about 1 mol of a monovalent metal cation. This capacity depends, of course, on local environmental conditions. Factors most impacting adsorption processes on clay mineral surfaces are pH and ionic strength. Depending on the chemical properties of the metal ions of interest, either one or both of these parameters can influence its overall retention (Box 2). For example, adsorption of alkaline and alkaline-earth metal ions in their cationic form such as rubidium (Rb^+)^{ref 16–19}, cesium (Cs^+)^{ref 20,21}, strontium (Sr^{2+})^{ref 22,23}, and barium (Ba^{2+})^{ref 19} is little impacted by pH, and strongly depends on ionic strength, while adsorption of more easily hydrolysed transition metals such as nickel (Ni^{2+})^{ref 24,25} and cobalt (Co^{2+})^{ref 26–28}, REEs, such as europium (Eu^{3+})^{ref 26,29}, and actinides^{ref 30}, such as uranium (UO_2^{2+})^{ref 29}, is affected by both parameters. Because adsorption can be a competitive process at surface sites, the chemical composition of the aqueous solution is also an important factor that contributes to the effectiveness of retention^{31–33}. Also, the presence of dissolved and adsorbed organic molecules can be beneficial or detrimental to metal ions adsorption on clay mineral surfaces^{22,34}.

Macroscopic quantification of cations retention on smectite and illite [G] surfaces amounts for countless studies in the literature (see references in³⁵) whereas studies concerning the retention of anionic species are more limited. Repulsive electrostatic interactions are responsible for anions repelling from the surface, and thus many anionic element do not sorb substantially on illite and montmorillonite surfaces, such as iodide (I^-), pertechnetate (TcO_4^-), and selenate (SeO_4^{2-})^{ref 36,37}. Some anions, including metalloids, sorb weakly, but notably, such as selenite (SeO_3^{2-})^{ref 36,38–41}, arsenate (AsO_4^{3-})^{ref 42–45}, arsenite (AsO_3^{3-}), antimony (in the forms $\text{Sb}(\text{OH})_3$ or $\text{Sb}(\text{OH})_6^-$)^{ref 46}, and molybdate (MoO_4^{2-})^{ref 47}. Adsorption dependences on environmental parameters are also different, often opposite, for anions compared to cations. For example, SeO_3^{2-} adsorption decreases with increasing pH, but is independent of ionic strength. For AsO_4^{3-} , adsorption on illite and montmorillonite increases up to pH 5-6 and then decreases at higher pH. Because adsorption of anions is much less efficient than of cations, clay materials are not often studied as promising materials for applications relying on anion retention properties such as pollution control engineering. This statement must be however reconsidered if modifications of clay mineral surface properties are obtained through interactions with organic molecules. So-called organo-clay materials have proven to be very effective in removing oxyanions such as hexavalent chromium (CrO_4^{2-})^{ref 48}. This Review is focused on interactions of metal ions with unmodified clay materials. Consequently, it is also mostly focused on interactions with metal cations.

The reasons for these differences among cations, as well as between cations and anions, were early ascribed to differences in interaction mechanisms on basal and edge surfaces with two main mechanisms⁴⁹ (Figure 2). The first one is **inner-sphere complex [G]** reactions, in which metal ions compete with protons (H^+) for the adsorption sites on edge surfaces, and the second is cation exchange reaction, in which metal ions replace layer charge compensating cations on

basal surfaces through, mostly, **outer-sphere complexes** [G]. Anions can also bind through ligand exchange [G] to form inner-sphere complex and in that case anions compete with edge hydroxyl and water surface groups. Because of the non-linearity of cation adsorption isotherms, it was soon necessary to subdivide edge surface complexation sites into two categories, the so-called strong and weak sites⁵⁰, which made it possible to account for the higher affinity of some metal ions for the surface at low equilibrium concentration. Competitive adsorption experiments³³ evidenced the need to define sub-categories of strong sites, meaning sites that are least abundant but most energetically favourable to retention, for which some metal ions do compete and some others do not.

Macroscopic observations of metal ion retention on clay mineral surfaces can be understood in principle by considering two main types of surface complexes on basal and edge surfaces. The rationale behind most of these macroscopic modelling concepts remains very empirical, but can be verified by progresses made in the molecular level view of the adsorption processes.

[H1] Molecular-level interaction mechanisms

Multiscale experimental and modeling approaches rooted in molecular level information (Box 3) are necessary to unravel the relative contributions of both the diverse array of metal ion retention mechanisms and the associated reactive sites on clay surfaces. Basal surfaces are terminated by saturated oxygen atoms whereas edge surfaces exhibit broken chemical bonds, leading thus in differences in reactivity between these two types of surfaces and metal ions. Hence, these interactions are discussed separately, and the influence of environmental parameters such as hydration state and the presence of organic matter are then introduced.

[H2] Basal surfaces

At basal surfaces, metal ions cannot form easily covalent bonding with surface atoms, which are already fully coordinated. Species adsorbed at basal surfaces are thus bound through weak long-range interactions such as electrostatics, which are the most effective for cations interacting with the negative potential created by the permanent negative charge of the layer. The adsorption state of cations largely depends on the Gibbs free energy of dehydration, that is, the cost in free energy of partial dehydration (such as, losing water ligand to form direct contact with the surface) makes the formation of inner-sphere complexes unfavourable. Therefore, most cations such as Li^+ , Na^+ and those of higher valences form outer-sphere complexes while K^+ , Rb^+ and Cs^+ form inner-sphere complexes due to lower dehydration free energy. The inner-sphere complexing sites include the positions above the center of ditrigonal cavity and above tetrahedron^{51–53}. Adsorbed cations compete with other cations present in solution, hence the dependence of adsorption on ionic strength and on background electrolyte composition⁵⁴.

The cation exchange thermodynamic theory makes it possible to conduct predictive quantifications without the need for molecular level understanding^{55,56}. It has however several

drawbacks including the difficulty to derive true thermodynamic equilibrium constants and activity coefficient of exchanged species⁵⁷. This problem often leaves exchange model parameters to the status of conditional constants that should not be applied without caution to conditions too different from the corresponding experimental conditions⁵⁸.

Cation exchange models can be enriched with the consideration of multiple sites present on a same clay mineral particle, and having contrasting affinities for metal ions adsorption. Cs⁺ exchange on illite surfaces represent certainly the best example for this need of a multiple sites description^{20,59,60}. Cs⁺ affinity for illite surface decreases by several order of magnitude with the increase of aqueous Cs⁺ equilibrium concentration. The presence of at least three types of exchange sites is necessary to explain this behaviour. The least abundant site must have also the highest affinity for Cs⁺ and is ascribed to the presence of so-called frayed edge sites⁶⁰, which correspond to adsorption sites on basal surfaces neighbouring the edge of illite particles⁶¹. The two other sites have been ascribed to illite basal surfaces as the sum of their capacities matches illite cation exchange capacity, but the reason for their contrasted affinities for Cs⁺ remains unclear⁶⁰. This example illustrates the underlying complexity of adsorption processes on basal surfaces.

Quantitative techniques in numerical simulation are now available to evaluate the profiles of cation adsorption free energy as functions of their distance from the basal clay mineral surfaces⁶², and these techniques can take into account the effects of layer charge distribution on these surfaces and distinguish between several specific adsorption sites⁵¹. Molecular simulations coupled to X-ray reflectivity and resonant anomalous X-ray reflectivity measurements provided evidence of the importance of interfacial water structure on the affinity of cations such as Rb⁺ and Cs⁺ for outer basal surfaces of phyllosilicates^{51,63,64}. Differences in the structure of water in the hydration shell lead to multiple adsorption positions for a single cation at a single surface, which could be a reason for the observed changes in macroscopic affinities as a function of cation concentration^{59,65–67}.

In interlayer domains of **swelling [G]** clay minerals, cations and their hydration sphere interact with both bordering inner basal surfaces⁶⁸. The layer-to-layer distance depends on the hydration of interlayer cations and on the external pressure applied to the clay-rich material⁶⁹. Conversely, experimental values of montmorillonite interlayer affinity for Cs⁺ increase with the pressure applied to the system, and hence with the change of interlayer occupancy from three water layers to two and one water layer(s)⁷⁰. According to molecular dynamics simulations and microcalorimetric experiments, the main driving force for Cs⁺ adsorption on clay mineral surface is not the a priori energetically favourable Cs⁺-clay mineral interaction, but the relative hydrophobicity of Cs⁺ compared to its cationic competitors for the surface^{51,52,64,71,72}. This molecular level information should help to build advanced cation exchange models that consider several energy terms to describe properly metal ions adsorption as a function of usual parameters such as concentrations, but also as a function of temperature, pressure and related hydration state encountered in underground clay-rich geological settings.

Most of the classical atomistic simulations of hydrated cation interactions with basal clay mineral surfaces only include the effects of molecular and ionic polarizability in an implicit

way through the effective parameters of interatomic interactions⁷³. However, more advanced models explicitly including the polarizability effects into calculations are also emerging^{74,75}.

Beyond the possibility to better describe and quantify metal ions affinity for basal surfaces, simulations and experiments at the molecular level offer a unique capability to study the mobility of surface species as a function of their location. The standard view of adsorbed surface species immobilized in the Stern layer is contradicted by evidences from molecular dynamics simulations^{76–79} and spectrometric measurements, such as nuclear magnetic resonance⁷⁹, which show substantial in-plane diffusion of species adsorbed on basal surfaces. Growing macroscopic experimental evidences about this coupling is also made available and macroscopic modelling of diffusive transport of metal ions in clay-rich materials has evolved accordingly since the early ~2010s' to take these coupled adsorption/diffusion processes fully into account^{14,80–82}, with important implications for the modelling of the performance of radioactive waste storage concepts in clay-rich geological formations^{83–85}. Because of the highly coupled nature of these processes, molecular level information is necessary to decipher the relative contributions of the various types of adsorbed species in interlayer, Stern layer and in the diffuse layer⁸⁶.

Because of the chemistry and structure of clay mineral layers, electrostatics is the dominating interaction at basal surface, making the formation of outer-sphere complex the major metal retention mechanism, except for cations having low dehydration free energy, which can be adsorbed as inner-sphere complexes. This apparent simplicity of interaction mechanism description is however hiding additional complexity arising from coupling with environmental parameters, such as pressure, or with other physical processes such as ion mobility.

[H2] Edge surfaces

Higher chemical reactivity leads to the higher diversity of interaction processes on edge surfaces. Surface complexation first occurs when edge groups gradually become available for complexing cations upon proton dissociation as pH increases. Further accumulation at higher pH can cause surface nucleation and crystal growth. In the meanwhile, interfacial electron transfer processes can participate in the interactions of redox-active metal ions with Fe-containing clay minerals.

[H3] Surface complexation

Clay minerals edge surface structure is responsible for a wide range of possible adsorption sites and processes, with adsorbates having the possibility to interact by surface complexation or ligand exchange with tetrahedral sites, octahedral sites or both, and by different binding modes such as mono- or multi-dentate surface complexes. Depending on the chemical nature of these sites (for example Al octahedra versus Mg or Fe octahedra), binding affinities with adsorbates can also vary. In addition, site coordination depends on the crystallographic plane of each edge, which adds up this complexity^{87–89}. The corresponding diversity of site types provides a reasonable explanation to the necessity to consider many sub-categories of edge adsorption

sites in surface complexation models. However, it highlights also the necessity to better constrain the nature of the surface complexation sites to understand competition processes.

Spectrometric techniques, such as X-ray absorption fine structure (EXAFS) spectroscopy, and diffractometric techniques, such as high-energy diffractometric methods, and more specifically differential X-ray pair distribution function (d-PDF), provide molecular level information to unravel retention processes on clay mineral edges. For example, d-PDF measurements evidenced the binding mode of Sb(V) on montmorillonite to be a bidentate complex attached to the edges of the octahedral sheet⁹⁰. While d-PDF can be used to decipher the crystallographic nature of surface complexation adsorption sites on clay minerals, some limitations of the technique prevent its general use in adsorption studies. These limitations include the needs of a high adsorbed concentration of the element of interest, and an a priori knowledge of the structure of clay mineral edges, which must remain unaffected during the experiment. Such limitations are partly circumvented by the use of EXAFS spectroscopy that allows determining and quantifying the local environment of adsorbed elements.

In experimental conditions identified as being favourable to surface complexation on strong sites Ni^{2+} adsorbs only in octahedral coordination in plane with the octahedral sheet on montmorillonite edges⁹¹. Adsorbed Zn exhibit a similar local environmental on montmorillonite strong edge sites. In conditions favourable to adsorption on weak sites, Zn had a more disordered configuration, possibly related to the presence of multiple adsorption sites, all being out of the clay mineral octahedral plane⁹² and possibly being bidentate complexes⁹³. For the adsorption of lanthanides, such as Eu, on illite and montmorillonite edge surfaces. Time-resolved laser fluorescence and EXAFS spectroscopy indicate the formation of inner-sphere surface complexes at $\text{pH} > 5$ for both clay minerals^{29,94,95, 192-194}. Correspondingly, surface complexation of Eu, other lanthanides and trivalent actinides on illite and montmorillonite can be modelled successfully with the same surface complexation model approach as that used for transition metals^{27,29,96}.

While diffractometric and spectrometric methods give insightful details about adsorption processes, they are often limited by the presence of multiple surface complexes that cannot be probed individually, and by the impossibility to distinguish a site configuration from another because of a lack of sensitivity of the method. This limitation can be overcome by coupling molecular level simulation predictions with diffractometric/spectrometric information. For example, the combination of FPMD simulations with EXAFS spectroscopy results made it possible to assign the outermost **dioctahedral [G]** vacancy of dioctahedral layers to strong sites for Zn^{2+} and 1st row transition metals^{93,97,98}, while other sites are related to weak sites, such as aluminol, silanol, apical oxygen and their combination⁹⁷ (see principle in Figure 3). Another interesting example is the complexation of uranyl on montmorillonite surfaces, for which different macroscopic modelling approaches yielded different interpretations about the binding mode and the sites available for this species^{99,100}, while being equally good at predicting available macroscopic retention observations as well as spectroscopic results. A possible physical basis was later provided by molecular level simulations. While multiple bidentate complexes were predicted by static density functional theory (DFT) calculations¹⁰¹⁻¹⁰³, first

principles molecular dynamics (FPMD) simulations showed that they have similar binding affinity and therefore can be treated with a single stability constant in a macroscopic surface complexation model¹⁰⁴. This example highlights that the determination of adsorption sites in case of surface complexation, both from microscopic and macroscopic points of view, is an extremely complex task, which requires the coupled use of several experimental and computational physical and chemical methods to obtain reliable results (Figure 3).

This identification of surface adsorption sites is made even more complicated in systems resembling to natural conditions with the possible interactions of aqueous components and surfaces in ternary (or more) surface complexes. The uranium-carbonate-montmorillonite case is very informative in this respect. This system has been investigated using EXAFS spectroscopy by several teams, yielding different interpretations of uranium binding mechanisms^{100,105,106}, with the reported presence¹⁰⁵ or absence¹⁰⁰ of ternary uranyl-carbonate-montmorillonite complexes for experiments conducted in similar conditions. Additional constraints provided by molecular level simulations of ternary complexes adsorption processes would certainly help to resolve this apparent inconsistency.

[H3] Nucleation and growth

At high pH values and in the presence of high concentrations of metal ions, surface complexes can serve as nucleation sites, thus promoting (co-)precipitation of metal ions. Epitaxial nucleation or growth has been found for the 1st row transition metal including Zn²⁺ ref 107,108, Ni²⁺ ref 109,110, Co²⁺ ref 111 and Fe²⁺ ref 112,113. The neoformed phases can be a phyllosilicate or a layered double hydroxide (LDH). LDH, similar to hydrotalcite, is made up of stacked octahedral layers, where the partial substitution of trivalent for divalent cations results in a positive layer charge, compensated by anions located in interlayer space. Because of structural similarities between the neoformed octahedral layer and the octahedral sheet of TOT layer, it is reasonable to assume that these phases nucleate and grow as a continuation of the edges (Figure 2). FPMD simulations¹¹⁴ evidenced that upon complexation in vacancy, these elements hydrolyse in normal pH range and thus provide complexing sites for subsequent metal cations, eventually yielding epitaxial nucleation. In contrast, cations with larger ionic radii like Pb²⁺ hardly hydrolyse on clay mineral surfaces, prohibiting the multinuclear complexation and nucleation. Phyllosilicates would form in presence of considerable amount of Si in solution, in laboratory as well as in natural systems^{12,108,115–117}. In samples from Zn-clay ores, transmission electron microscopy evidence was found for epitaxial growth of Zn-smectite from clay mineral edges which played a templating role¹¹⁸. FPMD study suggested that for the formation of phyllosilicates, the synchronous pathway (that is Si and metal ions co-precipitate at the same time, path G to H in Figure 2) is favourable over the stepwise pathway (that is the phyllosilicate is formed via silicification of neoformed hydroxide, path I to J in Figure 2)¹¹⁴.

Actinides and lanthanides can also form secondary mineral phases⁹⁴. Because of obviously larger ionic radii of f-elements, actinides and lanthanides cannot form phyllosilicate/hydroxide phase resembling the structure of clay minerals. In these cases, clay minerals might only provide complexing ligands, for example, in the formation of coffinite (U(IV)SiO₄), but have

no templating effect. Although classified as REEs together with lanthanides and Y, Sc can be incorporated into octahedral sheets, forming Sc-rich smectite¹¹⁹.

[H3] Surface redox reactions

Clay minerals often contain structural or adsorbed Fe^{ref 120}, which participate in electron transfer reaction with adsorbed redox sensitive metal ions¹²¹, such as U^{ref 122–124}, Np^{ref 124}, Pu^{ref 125,126}, Se^{ref 127,128}, Tc^{ref 124,129–131}, and Cr^{ref 131–135}. The mobility of redox sensitive elements depends on their oxidation state, often through the contrasted solubility and adsorption properties of oxidized and reduced aqueous species of a given element. The study of surface enhanced reduction or oxidation of redox sensitive metal ions is made very difficult by the numerous mechanisms that were identified as a function of the elements of interest, but also as a function of the nature of the clay mineral and of the geochemical conditions. For example, naturally reduced ferrous clay minerals from subsurface redox transition zones exhibit minimal reactivity towards the oxyanions TcO₄[−] and CrO₄^{2−} compared to those measured in previous studies on laboratory treated samples¹³¹. Their reduction capacity was enhanced by adsorbed Fe(II) although added Fe(II) was not detected as redox-reactive species within the outermost few nanometers of clay mineral surfaces. The adsorption of Se(IV) on montmorillonite is another example of a surface-enhanced redox reaction. In the presence of dissolved Fe(II) and in the pH range (pH < 8) where Fe(II) is also sorbed onto montmorillonite, a reductive precipitation of Se(IV) to nano-particulate Se(0) in the pH range (pH < 8) is observed^{127,136}. However, based on Mössbauer spectrometry and XANES measurements, Fe oxidation kinetic rate was much higher than Se reduction kinetic rate. Structural Fe(II) in a chemically reduced nontronite does not reduce As(V) or Sb(V), and when all structural Fe is Fe(III), it does not oxidize As(III) and Sb(III) neither. Also, Fe(III) within a Fe(II)–O–Fe(III) moiety is more reactive compared to that in Fe(III)–O–Fe(III) in oxidizing As(III) and Sb(III)^{ref 128,137}, and so, Fe(II)–O–Fe(III) moieties at the edge sites are assumed to be the redox-active species in Fe-containing clay minerals.

Electron transfer processes at mineral interfaces can in principles be modeled by using DFT based free energy calculation methods^{138,139}. However, the delocalization error caused by the poor description of the exchange energy in generalized gradient approximation (the commonly currently used DFT level) usually leads to errors in the estimates of redox levels and redox potentials, with the underestimate in redox potential reaching 1 eV¹⁴⁰. The estimate of redox levels and redox potentials could be improved to some extent by using the *beyond DFT technique*, such as Hubbard+U¹⁴¹ and constrained DFT¹⁴². These techniques have also been used to estimate the rate of self-exchange type electron transfer¹⁴³. However, such ad hoc tricks can bring about other problems. Advanced functionals such as hybrid/double-hybrid functional are able to obviously improve the predictions, for aqueous transition metal cations¹⁴⁴, liquid water¹⁴⁵ and solid-water interfaces¹⁴⁶. Unfortunately, FPMD using these functionals are easily tens of times more expensive than that with generalized gradient approximation. The computational cost has now been a major obstacle to the application on the mineral interfaces of geochemical/environmental interest. Understanding the redox properties and the associated electron transfer mechanisms in clay minerals is thus a key but also challenging issue on an experimental as well as from a computational point of view.

[H2] Influence of environmental parameters

[H3] Water saturation and surface hydration

Clay mineral surfaces are hydrated in conditions relevant to the critical zone. Water molecules are adsorbed through interactions with both adsorbed cations and clay surface atoms. A 43 % relative humidity is sufficient for external basal surface to be covered by a complete water layer, which corresponds to dry conditions in Earth's surficial environments. Relative humidity of only 0.2 % and 9 % are sufficient to establish fully hydrated smectite interlayer space with monolayer and double layer states respectively^{147,148} because of strong water attraction under nanosized confinement. Previous simulation and experimental studies indicate that under partially saturated conditions, outer-sphere complexes can transform into inner-sphere, that is, the adsorption is stronger compared to water saturated condition^{76,149}. On the opposite, adsorption of Cs⁺ on the outer-basal of montmorillonite decreases with decreasing water saturation levels in adjacent interlayer spaces⁶⁷, thus evidencing also possible long-range interactions influencing cation adsorption from one surface to another surface in clay mineral particles. This effect seems, however, to have a minor influence on cation mobility in clay-rich materials compared to the effect of pore connectivity decrease with decreasing water saturation levels¹⁵⁰.

[H3] Natural organic matter

In soil and sedimentary rock systems, the presence of organic matter brings in additional complexity on retention of metal elements¹⁵¹. Natural organic matter and clay minerals form organo-clay association through the bonding of active groups, such as carboxylate, phosphate, and ammonium groups, and hydrophobic interactions with aliphatic or aromatic moieties¹⁵². Organic matters can bind on outer basal and edge surfaces and can also intercalate into the interlayer region of clay minerals¹⁵³, with binding location and mechanism varying as a function of factors such as pH, ionic strength¹⁵².

Because of the multifunctionality of natural organic matter, they can alter surface hydrophilicity, cover surface sites while they bring in active groups which can serve as complexing sites for metal cations, and they can take part in interfacial electron transfer processes with redox-active groups¹⁵⁴. Consequently, the effect of organic matters on metal cation retention in clay-rich materials can be extremely complicated, and the presence of organics can promote or inhibit the retention of metal ions depending on investigated metals and experimental conditions^{22,34}.

The molecular-level mechanisms that are responsible for organic matter – metal ions – clay minerals interactions are still far from being fully understood. Natural organic matter are now described as supramolecular associations of a group of small molecules^{155,156} rather than macromolecules¹⁵⁷ or polymers¹⁵⁸, as evidenced by both experiments^{159,160} and molecular simulations¹⁶¹. By taking advantage of this new description of organic matter structure, molecular level models of organo-clay associations have been developed, which can explicitly take account of experimentally measured properties of organics and clay minerals^{162,163}. Such models together with multiscale simulation techniques can thus serve as a starting point to

explore microscopic interactions and develop predictive approaches for multicomponent systems.

Clay mineral edge surface reactivity is responsible for very diverse interaction processes with metal cations, including surface complexation, co-precipitation and redox reactions, which cannot be unravelled on the basis of batch chemical characterization only. Because the kinetics, reversibility, and thus efficiency of these retention processes are not the same depending on environmental conditions, deciphering their respective contributions is necessary to make useful predictions for industrial and environmental applications. Multiscale experimental and modeling approaches rooted in molecular level information have proved to be effective to do so (Figure 3), but many technical challenges remain, especially to model crystal growth and redox reactivity.

[H1] Industrial and environmental implications

Major advances in the ability to characterize and model interaction processes and mechanisms have important practical applications to several environmental and industrial processes. Below we briefly describe the current understanding of clay mineral-metal ion retention processes in both metallic waste pollution control and REE ion-adsorption deposits as examples.

[H2] Pollution control engineering

Clay minerals have exceptional thermal, mechanical, hydraulic and chemical properties, they are abundant in nature and reasonably cheap. Because of these features, clay-rich materials are commonly used as natural buffers to remediate contaminated soils and waters and to inhibit the migration of pollutants in disposal facilities for hazardous wastes including radioactive waste^{9,164–169}. Clay minerals are also increasingly finding new applications in materials science, biotechnology and clay mineral-based nanocomposites development^{166,170}.

Adsorption is one of the most efficient mechanisms to remove metal ions, which is why clay minerals have been used since the ~1970-1980s as a less toxic alternative for environmental remediation. However, in the face of increasing pollution from industrial and anthropogenic activities, increasing efforts have been made since the ~2000s to develop new types of clay mineral-based adsorbents modification of natural clay-rich material to increase its adsorption capacity, such as modified clay minerals and nanocomposites. Clay mineral-based adsorbents are used for the removal of toxic organic and inorganic (metal) contaminants from polluted waters. The removal efficiency of clay minerals towards pollutants can be increased through treatments of the material such as thermal and acid treatment, exfoliation, pillaring of cations, and modification with surfactants, polymers and organosilanes^{171–173}.

Clay mineral supported nanoparticle have high potential for use in the development of high-capacity adsorbents and photocatalyst. Montmorillonite supported zero-valent iron is very effective in removing highly toxic arsenic from aqueous solutions¹⁷⁴. The combination of many type of modification and the use of clay minerals of various morphologies (tubed, fibrous,

stacked) has led to the development to tailored made clay mineral based nanomaterial(s) with extreme high and selective adsorption properties^{175–177}. For instance, polymer-functionalized clay mineral nanocomposites combine the remarkable features of both nanoparticles and polymers. The use of clay mineral as a nanofillers in polymer matrixes confer the polymer desirable interfacial properties^{178,179}.

Most studies published in the field of pollution control engineering focus on aqueous contaminant removal efficiency of raw and treated clay-rich materials, and on the associated favorable environmental or engineered conditions. In proportion of the total number of studies, few gain insights from basic molecular understanding about retention processes. Notable exceptions to this dominant empiricism driven approach are found in the areas of radioactive waste storage^{9,180}, and of the study of mobility of metals in soils^{59,181,182}, for which cation exchange, surface complexation, surface precipitations, electron transfer, as well as interactions with natural organic matters have been identified as important clay mineral related processes in the understanding of metals mobility and biogeochemical cycling.

Geological disposal, which is presently the internationally preferred option for the storage of radioactive waste, relies on a multi-barrier concept, which is a combination of engineered barriers (waste form and canister, backfill, seal) and natural barriers (host rock), to ensure the containment and long-term isolation of the highly radio- and chemo- toxic waste from the biosphere. Clay minerals are key components of such most multi-barrier systems. The retention of (radio-)contaminants on clay minerals surfaces along potential transport paths is the main retardation mechanisms on which the safety assessment of deep geological repositories relies (Figure 3).

Because of the time- and length scales envisioned for radioactive waste storage, the prediction of contaminant migration in performance and safety assessments are commonly based on models using a limited set of macroscopic parameters, on which sensitivity analysis are conducted. These macroscopic parameters loop together many basic processes (Figure 3). For example, all retention mechanisms explored in this review are often up-scaled in the form of a single numerical parameter for a given radionuclide. In this respect, the safety case must demonstrate a detailed understanding of the physical–chemical phenomena governing retention processes, in order to confirm the consistency of the chosen up-scaling approach⁹ (Figure 3).

Retardation factors (R_f), which quantify the delayed aqueous transport of adsorbed contaminants compared to a perfect tracer, are major input parameters in performance and safety assessments⁸³. R_f values for strongly adsorbing tracers are commonly derived from K_D values measured from batch adsorption experiments. Since the ~2000s, evidence of coupled transport-retention processes through surface-enhanced diffusion have accumulated, which questions the adequacy of this equivalence between real R_f values and R_f values derived from batch K_D values. Related experimental and modelling study at all scales from molecular level^{15,81} to in situ tests^{183–185} gave rise to changes in modelling paradigms with consideration of emergent coupled processes^{82,83}, in which part of adsorbed species is not immobilized on the surface, but, on the contrary, participates to an enhancement of the overall diffusion flux^{186–188}. Adsorption must be seen as a process that both slows down metal ion transfer because of

accumulation on the surface, and also that accelerates their transfer through surface-enhanced diffusion. Consequently, a detailed understanding of adsorption process must be made available to use retention parameters obtained in static systems for the prediction of contaminants diffusive mobility.

[H2] Ion-adsorption REE ores

REEs ion-adsorption type deposits (IADs) have been known as an important source of REEs in the world in particular for heavy REEs^{189–194}. IADs are characterised by high recovery rate of REEs simply by leaching of REEs with an ammonium sulphate solution at normal temperature, and low leachable amounts of U and Th, which can cause problems in other REEs sources in terms of environmental problems and working environment. Thus, IADs are ideal REE resources, which are critical to society due to its use in modern technologies^{195,196}.

IADs are mainly found in weathered profile of felsic igneous rocks with a variety of clay minerals. In most cases, weathered granite has been developed, but IADs can also be found in felsic volcanic rocks in the world^{191,193,197–199}. IADs typically consist of a strongly weathered zone at the surface layer, and an enriched zone of REEs in the subsurface layer accumulated mainly by adsorption through outer-sphere complexation of hydrated REE trivalent cation to clay minerals (Figure 4a,b)^{189,199,200}. The surface layer exhibits a positive Ce anomaly in REE patterns due to the removal of the other REEs and fixation of Ce by its oxidation to insoluble Ce(IV) species^{201,202}, whereas the subsurface REE-enriched layer generally shows a negative Ce anomaly due to the fixation of REEs, except for Ce (Figure 4c-e).

REE species in the enriched zone have been revealed by EXAFS spectroscopy^{189,200}, showing that the outer-sphere surface complex to clay minerals is main REE species, and the species is responsible for the high recovery rate of REE by the ion-exchange reaction^{192,203}. These results are consistent with laboratory studies on the formation of outer-sphere complex to various clay minerals, such as montmorillonite, as evidenced by EXAFS spectroscopy^{189,200,204} and by laser-induced fluorescence spectroscopy^{205,206}. The enriched zones are usually located in acidic environment ($\text{pH} < 6$)¹³⁸. The lower pH is unfavorable for dissociation of groups of edge surfaces, thus suppressing the formation of REE inner-sphere complexes. Although the identification of phyllosilicates at the nm-scale is possible by transmission electron microscopy, the detection of REEs in the same view presented a challenge, which inhibited the attainment of clear identification of the REE host phase. In such cases, secondary ion mass spectrometry (SIMS) can bring additional insights²⁰⁷. Identification of the host mineral is primarily important, since the type of host mineral is related to the degree of weathering depending on temperature and rainfall²⁰⁸, which is crucial information for the survey of IADs, and the recovery rate of REE from the IADs.

High REEs extractable property of IADs is very contrastive to marine REEs resources such as marine ferromanganese oxides with low extractability of REEs ($< 1\%$) due to the formation of inner-sphere surface complex of REEs^{209–212} and deep-sea REEs-rich mud with REEs incorporated as phosphate phases²¹³. However, IADs cannot be formed under marine environment due to high salinity of seawater, which shows that IADs are specific to land areas.

The difference between IADs and marine ferromanganese oxides originated from the different REE retention mechanisms: the former is mainly through electrostatics which is hindered by high ionic strength, whereas the latter is through chemical bonding. This example clearly shows that molecular-level studies allow systematic understanding of ion retention that occurs in natural systems, and to develop its application such as extraction of useful metals.

Retention reversibility and adsorbed cation mobility are two key aspects of resources extraction efficiency in industrial processes and contaminant mobility in pollution control engineering. Both properties are linked with the speciation of metal cations at clay mineral surfaces, with the presence of outer-sphere complexes enhancing reversibility and mobility.

[H1] Summary and future directions

The accurate predictions of metal ion – clay mineral interactions over long time- and large-spatial scales in natural and engineered systems necessitates the development of a continuum of macroscopic models that are able to consider a large range of environmental conditions, as well as temporal and spatial changes. Such predictions are currently hampered by the diversity of interaction processes of metal ions with clay mineral surfaces, and by the difficulty to unravel their respective contributions in the results of macroscopic experiments that are used to calibrate retention models, such as surface complexation models. This limitation is currently being addressed by implementing retention models with molecular level characterization to better understand adsorption and related processes.

The highly complex nature of clay mineral-metal ion interactions requires the application of multiple techniques to reach insightful conclusions. Important progress has been made since the ~2000s in this direction, with important breakthroughs in deciphering mechanisms of adsorption and of incorporation of elements, with applications to the formation mechanisms of economically important metal deposits, as well as to the containment of hazardous materials by clay-rich barriers. Since the 2010s, the emerging coupling of quantum mechanics simulation predictions with molecular level synchrotron-based characterization techniques proved to be very powerful to better constrain the nature and location of adsorption sites, binding mechanisms, as well as the energy associated to binding reactions, thus allowing further development of macroscopic models with a reduced number of empirically fitted parameters. It is now also possible to obtain quantified information on surface nucleation and growth mechanisms that are yet not integrated into geochemical modelling approaches.

With the application of higher quantum mechanical levels (such as advanced density functional and perturbation theory), more accurate estimates can be made, approaching chemical accuracy (about 1 kJ mol⁻¹). Multiscale modelling will allow the system size and time scale to be expanded substantially towards ~μm and ~s respectively, enabling the direct simulation of slow processes, such as nucleation and dissolution, and promoting the combination with experimental results. Therefore, one can expect that the continuous development of efficient algorithms and increases in computing power will greatly advance the predictive capability of

microscopic simulation, which is going to play an ever more important role in guiding industrial and engineering applications.

Concerning adsorption processes, the quantification of surface ternary complex formation (in particular, in the presence of carbonated metal ions species) and a better understanding of metal-organic matter-clay mineral surface interactions, are needed to model conditions relevant to natural systems. Surface nucleation and growth clearly deserves more mechanistic research for their fundamental importance in both pollution control engineering and transition metal enriched clay deposits, such as zinc clay ores¹¹⁸ and nickel laterite ores²¹⁴.

Surface induced redox reactions have important implications for the containment performance of engineered and natural clay-rich barriers in pollution control applications, but also for bioremediation applications. The detailed understanding of surface induced redox reactions with respect to the retention of redox sensitive metals still requires extensive research before implementation in geochemical models, particularly with respect to the redox properties of iron. In particular, further research is needed for the identification of electron transfer paths and efficiency; for the assessment and thermodynamic description of intrinsic redox potential of structural and adsorbed Fe; for the identification of relationship between changes in Fe oxidation state and surface chemistry; and, for the quantification of Fe redox reactivity as a function of its abundance and location in the crystal structure.

The growing scientific interest in the quantification and understanding of clay mineral retention properties must be put in perspective with industrial and environmental applications that rely on the ability of clay minerals to scavenge metal ions. Bulk characterization of retention properties is necessary to study the effectiveness of clay-rich materials for such applications, but still is not sufficient to quantify these processes over long timescales. Process understanding at the molecular level combined with multiscale simulation approaches has proved to be essential to predict parameters such as resource extractability and contaminant mobility.

References:

- 594 1. Bergaya, F. & Lagaly, G. *Handbook of clay science, second edition. 1 and 2*, (Elsevier:
595 2013).
- 596 2. Sposito, G., Skipper, N. T., Sutton, R., Park, S. & Soper, A. K. Surface geochemistry of the
597 clay minerals. *Proceedings of the National Academy of Sciences of the United States of*
598 *America* **96**, 3358–3364 (1999).
- 599 3. Li, M. Y. H. & Zhou, M.-F. The role of clay minerals in formation of the regolith-hosted
600 heavy rare earth element deposits. **105**, 92–108 (2020).
- 601 4. Delay, J., Distinguin, M. & Dewonck, S. Characterization of a clay-rich rock through
602 development and installation of specific hydrogeological and diffusion test equipment
603 in deep boreholes. *Physics and Chemistry of the Earth, Parts A/B/C* **32**, 393–407 (2007).
- 604 5. Mishra, H., Karmakar, S., Kumar, R. & Kadambala, P. A long-term comparative
605 assessment of human health risk to leachate-contaminated groundwater from heavy
606 metal with different liner systems. **25**, 2911–2923 (2018).
- 607 6. Yi, X. *et al.* Remediation of heavy metal-polluted agricultural soils using clay minerals: a
608 review. **27**, 193–204 (2017).
- 609 7. Brigatti, M. F., Galán, E. & Theng, B. K. G. Chapter 2 - Structure and Mineralogy of Clay
610 Minerals. *Handbook of Clay Science* **5**, 21–81 (2013).
- 611 8. Yuan, G. D., Theng, B. K. G., Churchman, G. J. & Gates, W. P. Chapter 5.1 - Clays and Clay
612 Minerals for Pollution Control. *Handbook of Clay Science* **5**, 587–644 (2013).
- 613 9. Altmann, S. Geochemical research: A key building block for nuclear waste disposal
614 safety cases. *Journal of Contaminant Hydrology* **102**, 174–179 (2008).
- 615 10. Skipper, N., Soper, A. & McConnell, J. The structure of interlayer water in vermiculite.
616 **94**, 5751–5760 (1991).
- 617 11. Schlegel, M. L. *et al.* Cation sorption on the muscovite (0 0 1) surface in chloride
618 solutions using high-resolution X-ray reflectivity. *Geochimica et Cosmochimica Acta* **70**,
619 3549–3565 (2006).
- 620 12. Dähn, R. *et al.* Neoformation of Ni phyllosilicate upon Ni uptake on montmorillonite: a
621 kinetics study by powder and polarized extended X-ray absorption fine structure
622 spectroscopy. *Geochimica et Cosmochimica Acta* **66**, 2335–2347 (2002).
- 623 13. Manceau, A. & Calas, G. Nickel-bearing clay minerals: II. Intracrystalline distribution of
624 nickel: an X-ray absorption study. **21**, 341–360 (1986).
- 625 14. Churakov, S. V. & Prasianakis, N. I. Review of the current status and challenges for a
626 holistic process-based description of mass transport and mineral reactivity in porous
627 media. *American Journal of Science* **318**, 921–948 (2018).
- 628 15. Churakov, S. V. & Gimmi, T. Up-scaling of molecular diffusion coefficients in clays: A two-
629 step approach. *The Journal of Physical Chemistry C* **115**, 6703–6714 (2011).
- 630 16. Brouwer, E., Baeyens, B., Maes, A. & Cremers, A. Cesium and Rubidium ion equilibria in
631 illite clay. *Journal of Physical Chemistry* **87**, 1213–1219 (1983).
- 632 17. De Koning, A. & Comans, R. N. J. Reversibility of radiocaesium sorption on illite.
633 *Geochimica et Cosmochimica Acta* **68**, 2815–2823 (2004).

18. Poinssot, C., Baeyens, B. & Bradbury, M. H. *Experimental studies of Cs, Sr, Ni, and Eu sorption on Na-illite and the modelling of Cs sorption*. (Paul Scherrer Institut: 1999).
19. Verburg, K. & Baveye, P. Hysteresis in the binary exchange of cations on 2/1 clay-minerals - a critical-review. *Clays and Clay Minerals* **42**, 207–220 (1994).
20. Comans, R. N. J., Haller, M. & De Preter, P. Sorption of cesium on illite: Non-equilibrium behaviour and reversibility. *Geochimica et Cosmochimica Acta* **55**, 433–440 (1991).
21. Oscarson, D. W., Hume, H. B. & King, F. Sorption of cesium on compacted bentonite. *Clays and Clay Minerals* **42**, 731–736 (1994).
22. Bellenger, J. P. & Staunton, S. Adsorption and desorption of Sr-85 and Cs-137 on reference minerals, with and without inorganic and organic surface coatings. *Journal of Environmental Radioactivity* **99**, 831–840 (2008).
23. Dyer, A., Chow, J. K. & Umar, I. M. The uptake of caesium and strontium radioisotopes onto clays. *Journal of Materials Chemistry* **10**, 2734–2740 (2000).
24. Baeyens, B. & Bradbury, M. H. A mechanistic description of Ni and Zn sorption on Na-montmorillonite. Part I: Titration and sorption measurements. *Journal of Contaminant Hydrology* **27**, 199–222 (1997).
25. Gu, X. & Evans, L. J. Modelling the adsorption of Cd(II), Cu(II), Ni(II), Pb(II), and Zn(II) onto Fithian illite. *Journal of Colloid and Interface Science* **307**, 317–325 (2007).
26. Bradbury, M. H. & Baeyens, B. Sorption modelling on illite Part I: Titration measurements and the sorption of Ni, Co, Eu and Sn. *Geochimica et Cosmochimica Acta* **73**, 990–1003 (2009).
27. Bradbury, M. H. & Baeyens, B. Modelling the sorption of Mn(II), Co(II), Ni(II), Zn(II), Cd(II), Eu(III), Am(III), Sn(IV), Th(IV), Np(V) and U(VI) on montmorillonite: Linear free energy relationships and estimates of surface binding constants for some selected heavy metals and actinides. *Geochimica et Cosmochimica Acta* **69**, 875–892 (2005).
28. Akafia, M. M., Reich, T. J. & Koretsky, C. M. Assessing Cd, Co, Cu, Ni, and Pb Sorption on montmorillonite using surface complexation models. *Applied geochemistry* **26**, S154–S157 (2011).
29. Marques Fernandes, M., Scheinost, A. & Baeyens, B. Sorption of trivalent lanthanides and actinides onto montmorillonite: Macroscopic, thermodynamic and structural evidence for ternary hydroxo and carbonato surface complexes on multiple sorption sites. *Water Research* **99**, 74–82 (2016).
30. Bradbury, M. H. & Baeyens, B. Sorption modelling on illite. Part II: Actinide sorption and linear free energy relationships. *Geochimica et Cosmochimica Acta* **73**, 1004–1013 (2009).
31. Bradbury, M. H. & Baeyens, B. Experimental measurements and modeling of sorption competition on montmorillonite. *Geochimica et Cosmochimica Acta* **69**, 4187–4197 (2005).
32. Grangeon, S. *et al.* The influence of natural trace element distribution on the mobility of radionuclides. The exemple of nickel in a clay-rock. *Applied Geochemistry* **52**, 155–173 (2015).
33. Marques Fernandes, M. & Baeyens, B. Cation exchange and surface complexation of lead on montmorillonite and illite including competitive adsorption effects. *Applied Geochemistry* **100**, 190–202 (2019).
34. Gao, Y., Shao, Z. & Xiao, Z. U (VI) sorption on illite: effect of pH, ionic strength, humic acid and temperature. *Journal of Radioanalytical and Nuclear Chemistry* **303**, 867–876 (2015).

35. Uddin, M. K. A review on the adsorption of heavy metals by clay minerals, with special focus on the past decade. *Chemical Engineering Journal* **308**, 438–462 (2017).
36. Goldberg, S. & Glaubig, R. A. Anion sorption on a calcareous, montmorillonitic soil-selenium. *Soil Science Society of America Journal* **52**, 954–958 (1988).
37. Palmer, D. A. & Meyer, R. E. Adsorption of technetium on selected inorganic ion-exchange materials and on a range of naturally occurring minerals under oxic conditions. *Journal of Inorganic and Nuclear Chemistry* **43**, 2979–2984 (1981).
38. Missana, T., Alonso, U. & Garcia-Gutiérrez, M. Experimental study and modelling of selenite sorption onto illite and smectite clays. *Journal of Colloid and Interface Science* **334**, 132–138 (2009).
39. Peak, D., Saha, U. & Huang, P. Selenite adsorption mechanisms on pure and coated montmorillonite: an EXAFS and XANES spectroscopic study. **70**, 192–203 (2006).
40. Ervanne, H., Hakanen, M. & Lehto, J. Selenium sorption on clays in synthetic groundwaters representing crystalline bedrock conditions. **307**, 1365–1373 (2016).
41. Goldberg, S. Modeling selenite adsorption envelopes on oxides, clay minerals, and soils using the triple layer model. **77**, 64–71 (2013).
42. Manning, B. A. & Goldberg, S. Adsorption and stability of arsenic(III) at the clay mineral-water interface. *Environmental Science & Technology* **31**, 2005–2011 (1997).
43. Garcia-Sanchez, A., Alvarez-Ayuso, E. & Rodriguez-Martin, F. Sorption of As (V) by some oxyhydroxides and clay minerals. Application to its immobilization in two polluted mining soils. **37**, 187–194 (2002).
44. Mohapatra, D., Mishra, D., Chaudhury, G. R. & Das, R. Arsenic (V) adsorption mechanism using kaolinite, montmorillonite and illite from aqueous medium. **42**, 463–469 (2007).
45. Goldberg, S. Competitive adsorption of arsenate and arsenite on oxides and clay minerals. **66**, 413–421 (2002).
46. Xi, J., He, M. & Lin, C. Adsorption of antimony (III) and antimony (V) on bentonite: kinetics, thermodynamics and anion competition. **97**, 85–91 (2011).
47. Goldberg, S., Forster, H. & Godfrey, C. Molybdenum adsorption on oxides, clay minerals, and soils. *Soil Science Society of America Journal* **60**, 425–432 (1996).
48. Lee, S. M. & Tiwari, D. Organo and inorgano-organo-modified clays in the remediation of aqueous solutions: An overview. *Applied Clay Science* **59**, 84–102 (2012).
49. Fletcher, P. & Sposito, G. The chemical modeling of clay/electrolyte interactions for montmorillonite. *Clay Minerals* **24**, 375–391 (1989).
50. Bradbury, M. H. & Baeyens, B. A mechanistic description of Ni and Zn sorption on Na-montmorillonite. Part II: modeling. *Journal of Contaminant Hydrology* **27**, 223–248 (1997).
51. Loganathan, N. & Kalinichev, A. G. Quantifying the mechanisms of site-specific ion exchange at an inhomogeneously charged surface: Case of Cs⁺/K⁺ on hydrated muscovite mica. *The Journal of Physical Chemistry C* **121**, 7829–7836 (2017).
52. Loganathan, N., Yazaydin, A. O., Bowers, G. M., Kalinichev, A. G. & Kirkpatrick, R. J. Structure, energetics, and dynamics of Cs⁺ and H₂O in hectorite: Molecular dynamics simulations with an unconstrained substrate surface. *The Journal of Physical Chemistry C* **120**, 10298–10310 (2016).
53. Liu, X., Lu, X., Wang, R. & Zhou, H. Effects of layer-charge distribution on the thermodynamic and microscopic properties of Cs-smectite. *Geochimica et Cosmochimica Acta* **72**, 1837–1847 (2008).

54. Tournassat, C., Grangeon, S., Leroy, P. & Giffaut, E. Modeling specific pH dependent sorption of divalent metals on montmorillonite surfaces. A review of pitfalls, recent achievements and current challenges. *American Journal of Science* **313**, 395–451 (2013).
55. Thomas, H. C. & Gaines, G. L. J. The thermodynamics of ion exchange on clay minerals. A preliminary report on the system montmorillonite-Cs-Sr. *Clays and Clay Minerals* **2**, 398–403 (1953).
56. Vanselow, A. P. The utilization of the base-exchange reaction for the determination of activity coefficients in mixed electrolytes. *Journal of American Chemical Society* **54**, 1307–1311 (1932).
57. Bourg, I. C. & Sposito, G. Ion exchange phenomena. *Handbook of Soil Science, second edition* (2011).
58. Tournassat, C. *et al.* Cation exchange selectivity coefficient values on smectite and mixed-layer illite/smectite minerals. *Soil Science Society of America Journal* **73**, 928–942 (2009).
59. Lammers, L. N. *et al.* Molecular dynamics simulations of cesium adsorption on illite nanoparticles. *Journal of Colloid and Interface Science* **submitted**, (2016).
60. Poinssot, C., Baeyens, B. & Bradbury, M. H. Experimental and modelling studies of caesium sorption on illite. *Geochimica et Cosmochimica Acta* **63**, 3217–3227 (1999).
61. Bergaoui, L., Lambert, J. F. & Prost, R. Cesium adsorption on soil clay: macroscopic and spectroscopic measurements. *Applied Clay Science* **29**, 23–29 (2005).
62. Meleshyn, A. Adsorption of Sr²⁺ and Ba²⁺ at the cleaved mica–water interface: Free energy profiles and interfacial structure. *Geochimica et Cosmochimica Acta* **74**, 1485–1497 (2010).
63. Bourg, I. C., Lee, S. S., Fenter, P. & Tournassat, C. Stern Layer Structure and Energetics at Mica–Water Interfaces. *The Journal of Physical Chemistry C* **121**, 9402–9412 (2017).
64. Zaunbrecher, L. K., Cygan, R. T. & Elliott, W. C. Molecular models of cesium and rubidium adsorption on weathered micaceous minerals. *The Journal of Physical Chemistry A* **119**, 5691–5700 (2015).
65. Rotenberg, B., Marry, V., Malikova, N. & Turq, P. Molecular simulation of aqueous solutions at clay surfaces. *Journal of Physics: Condensed Matter* **22**, 284114 (2010).
66. Tournassat, C., Chapron, Y., Leroy, P. & Boulahya, F. Comparison of molecular dynamics simulations with Triple Layer and modified Gouy-Chapman models in a 0.1 M NaCl - montmorillonite system. *Journal of Colloid and Interface Science* **339**, 533–541 (2009).
67. Li, X., Liu, N. & Zhang, J. Adsorption of cesium at the external surface of TOT type clay mineral: effect of the interlayer cation and the hydrated state. **123**, 19540–19548 (2019).
68. Tournassat, C., Bourg, I. C., Steefel, C. I. & Bergaya, F. Chapter 1 - Surface Properties of Clay Minerals. *Natural and Engineered Clay Barriers* **6**, 5–31 (2015).
69. Liu, L. Prediction of swelling pressures of different types of bentonite in dilute solutions. *Colloids and Surfaces A: Physicochemical and Engineering Aspects* **434**, 303–318 (2013).
70. Van Loon, L. R. & Glaus, M. A. Mechanical compaction of smectite clays increases ion exchange selectivity for cesium. *Environmental Science & Technology* **42**, 1600–1604 (2008).
71. Rotenberg, B., Morel, J.-P., Marry, V., Turq, P. & Morel-Desrosiers, N. On the driving force of cation exchange in clays: Insights from combined microcalorimetry experiments and molecular simulation. *Geochimica et Cosmochimica Acta* **73**, 4034–4044 (2009).

72. Teppen, B. J. & Miller, D. M. Hydration energy determines isovalent cation exchange selectivity by clay minerals. *Soil Science Society of America Journal* **70**, 31–40 (2006).
73. Cygan, R. T., Greathouse, J. A. & Kalinichev, A. G. Advances in Clayff molecular simulation of layered and nanoporous materials and their aqueous interfaces. **125**, 17573–17589 (2021).
74. Le Crom, S., Tournassat, C., Robinet, J.-C. & Marry, V. Influence of polarisability on the prediction of the electrical double layer structure in a clay mesopore: A molecular dynamics study. *The Journal of Physical Chemistry C* **124**, 6221–6232 (2020).
75. Tesson, S. *et al.* Classical polarizable force field to study hydrated charged clays and zeolites. **122**, 24690–24704 (2018).
76. Churakov, S. V. Mobility of Na and Cs on montmorillonite surface under partially saturated conditions. *Environmental Science & Technology* **47**, 9816–9823 (2013).
77. Simonnin, P., Marry, V., Noetinger, B., Nieto-Draghi, C. & Rotenberg, B. Mineral-and ion-specific effects at clay–water interfaces: structure, diffusion, and hydrodynamics. *The Journal of Physical Chemistry C* **122**, 18484–18492 (2018).
78. Malikova, N., Dubois, E., Marry, V., Rotenberg, B. & Turq, P. Dynamics in clays-combining neutron scattering and microscopic simulation. **224**, 153–181 (2010).
79. Porion, P. *et al.* 133Cs Nuclear Magnetic Resonance relaxometry as a probe of the mobility of cesium cations confined within dense clay sediments. **119**, 15360–15372 (2015).
80. Appelo, C. A. J., Van Loon, L. R. & Wersin, P. Multicomponent diffusion of a suite of tracers (HTO, Cl, Br, I, Na, Sr, Cs) in a single sample of Opalinus clay. *Geochimica et Cosmochimica Acta* **74**, 1201–1219 (2010).
81. Churakov, S. V., Gimmi, T., Unruh, T., Van Loon, L. R. & Juranyi, F. Resolving diffusion in clay minerals at different time scales: Combination of experimental and modeling approaches. *Applied Clay Science* (2014).
82. Tournassat, C. & Steefel, C. I. Reactive transport modeling of coupled processes in nanoporous media. *Reviews in Mineralogy and Geochemistry* **85**, 75–110 (2019).
83. Altmann, S. *et al.* Diffusion-driven transport in clayrock formations. *Applied Geochemistry* **27**, 463–478 (2012).
84. Charlet, L., Alt-Epping, P., Wersin, P. & Gilbert, B. Diffusive transport and reaction in clay rocks: A storage (nuclear waste, CO₂, H₂), energy (shale gas) and water quality issue. *Advances in Water Resources* **106**, 39–59 (2017).
85. Grambow, B. Geological disposal of radioactive waste in clay. *Elements* **12**, 239–245 (2016).
86. Whittaker, M. L., Lammers, L. N., Carrero, S., Gilbert, B. & Banfield, J. F. Ion exchange selectivity in clay is controlled by nanoscale chemical–mechanical coupling. *Proceedings of the National Academy of Sciences* **116**, 22052–22057 (2019).
87. Liu, X., Cheng, J., Sprik, M., Lu, X. & Wang, R. Interfacial structures and acidity of edge surfaces of ferruginous smectites. *Geochimica et Cosmochimica Acta* **168**, 293–301 (2015).
88. Liu, X., Cheng, J., Sprik, M., Lu, X. & Wang, R. Surface acidity of 2:1-type dioctahedral clay minerals from first principles molecular dynamics simulations. *Geochimica et Cosmochimica Acta* **140**, 410–417 (2014).
89. Liu, X. *et al.* Acidity of edge surface sites of montmorillonite and kaolinite. *Geochimica et Cosmochimica Acta* **117**, 180–190 (2013).

90. Genuchten, C. M. van & Peña, J. Antimonate and arsenate speciation on reactive soil minerals studied by differential pair distribution function analysis. *Chemical Geology* **429**, 1–9 (2016).
91. Dähn, R. *et al.* Structural evidence for the sorption of Ni(II) atoms on the edges of montmorillonite clay minerals: A polarized X-ray absorption fine structure study. *Geochimica et Cosmochimica Acta* **37**, 1–15 (2003).
92. Dähn, R., Baeyens, B. & Bradbury, M. H. Investigation of the different binding edge sites for Zn on montmorillonite using P-EXAFS - The strong/weak site concept in the 2SPNE SC/CE sorption model. *Geochimica et Cosmochimica Acta* **75**, 5154–5168 (2011).
93. Churakov, S. V. & Dähn, R. Zinc Adsorption on Clays Inferred from Atomistic Simulations and EXAFS Spectroscopy. *Environmental Science & Technology* **46**, 5713–5719 (2012).
94. Rabung, T. *et al.* Sorption of Eu(III)/Cm(III) on Ca-montmorillonite and Na-illite. Part 1: Batch sorption and time-resolved laser fluorescence spectroscopy experiments. *Geochimica et Cosmochimica Acta* **69**, 5393–5402 (2005).
95. Sasaki, T. *et al.* Sorption of Eu³⁺ on Na-montmorillonite studied by time-resolved laser fluorescence spectroscopy and surface complexation modeling. *Journal of Nuclear Science and Technology* **53**, 592–601 (2016).
96. Verma, P. K. *et al.* Eu (III) sorption onto various montmorillonites: Experiments and modeling. *Applied Clay Science* **175**, 22–29 (2019).
97. Zhang, C. *et al.* Cadmium (II) complexes adsorbed on clay edge surfaces: Insight from first principles molecular dynamics simulation. *Clays and Clay Minerals* **64**, 337–347 (2016).
98. Zhang, C. *et al.* Surface complexation of heavy metal cations on clay edges: insights from first principles molecular dynamics simulation of Ni (II). *Geochimica et Cosmochimica Acta* **203**, 54–68 (2017).
99. Tournassat, C., Tinnacher, R. M., Grangeon, S. & Davis, J. A. Modeling uranium (VI) adsorption onto montmorillonite under varying carbonate concentrations: A surface complexation model accounting for the spillover effect on surface potential. *Geochimica et Cosmochimica Acta* **220**, 291–308 (2018).
100. Marques Fernandes, M., Baeyens, B., Dähn, R., Scheinost, A. & Bradbury, M. U(VI) sorption on montmorillonite in the absence and presence of carbonate: A macroscopic and microscopic study. **93**, 262–277 (2012).
101. Kremleva, A., Martorell, B., Krüger, S. & Rösch, N. Uranyl adsorption on solvated edge surfaces of pyrophyllite: a DFT model study. *Physical Chemistry Chemical Physics* **14**, 5815–5823 (2012).
102. Kremleva, A., Krüger, S. & Rösch, N. Uranyl adsorption at solvated edge surfaces of 2: 1 smectites. A density functional study. *Physical Chemistry Chemical Physics* **17**, 13757–13768 (2015).
103. Kremleva, A., Krüger, S. & Rösch, N. Toward a reliable energetics of adsorption at solvated mineral surfaces: A computational study of uranyl (VI) on 2: 1 clay minerals. *The Journal of Physical Chemistry C* **120**, 324–335 (2016).
104. Zhang, C., Liu, X., Tinnacher, R. M. & Tournassat, C. Mechanistic understanding of uranyl ion complexation on montmorillonite edges: A combined first-principles molecular dynamics - surface complexation modeling approach. *Environmental Science & Technology* **52**, 8501–8509 (2018).

105. Catalano, J. G. & Brown, G. E. Jr. Uranyl adsorption onto montmorillonite: Evaluation of binding sites and carbonate complexation. *Geochimica et Cosmochimica Acta* **69**, 2995–3005 (2005).
106. Schlegel, M. L. & Descostes, M. Uranium uptake by hectorite and montmorillonite: a solution chemistry and polarized EXAFS study. *Environmental Science & Technology* **43**, 8593–8598 (2009).
107. Ford, R. G. & Sparks, D. L. The nature of Zn precipitates formed in the presence of pyrophyllite. *Environmental Science and Technology* **34**, 2479–2483 (2000).
108. Schlegel, M. L. & Manceau, A. Evidence for the nucleation and epitaxial growth of Zn phyllosilicate on montmorillonite. *Geochimica et Cosmochimica Acta* **70**, 901–917 (2006).
109. Scheidegger, A. M., Lamble, G. M. & Sparks, D. L. Spectroscopic evidence for the formation of mixed-cation hydroxide phases upon metal sorption on clays and aluminum oxides. *Journal of Colloid and Interface Science* **186**, 118–128 (1997).
110. Siebecker, M., Li, W., Khalid, S. & Sparks, D. Real-time QEXAFS spectroscopy measures rapid precipitate formation at the mineral–water interface. *Nature communications* **5**, 1–7 (2014).
111. Thompson, H. A., Parks, G. A. & Brown Jr., G. E. Dynamic interactions of dissolution, surface adsorption, and precipitation in an aging cobalt(II)-clay-water system. *Geochimica et Cosmochimica Acta* **63**, 1767–1779 (1999).
112. Starcher, A. N., Li, W., Kukkadapu, R. K., Elzinga, E. J. & Sparks, D. L. Fe (II) sorption on pyrophyllite: Effect of structural Fe (III)(impurity) in pyrophyllite on nature of layered double hydroxide (LDH) secondary mineral formation. *Chemical Geology* **439**, 152–160 (2016).
113. Zhu, Y. & Elzinga, E. J. Formation of layered Fe(II)-hydroxides during Fe(II) sorption onto clay and metal-oxide substrates. *Environmental science & technology* **48**, 4937–4945 (2014).
114. Zhang, C., Liu, X., Lu, X., Meijer, E. J. & Wang, R. Understanding the Heterogeneous Nucleation of Heavy Metal Phyllosilicates on Clay Edges with First-Principles Molecular Dynamics. *Environmental science & technology* **53**, 13704–13712 (2019).
115. Jacquat, O., Voegelin, A., Villard, A., Marcus, M. A. & Kretzschmar, R. Formation of Zn-rich phyllosilicate, Zn-layered double hydroxide and hydrozincite in contaminated calcareous soils. *Geochimica et Cosmochimica Acta* **72**, 5037–5054 (2008).
116. Choulet, F., Buatier, M., Barbanson, L., Guégan, R. & Ennaciri, A. Zinc-rich clays in supergene non-sulfide zinc deposits. *Mineralium Deposita* **51**, 467–490 (2016).
117. Roqué-Rosell, J., Villanova-de-Benavent, C. & Proenza, J. A. The accumulation of Ni in serpentines and garnierites from the Falcondo Ni-laterite deposit (Dominican Republic) elucidated by means of μ XAS. *Geochimica et Cosmochimica Acta* **198**, 48–69 (2017).
118. Balassone, G., Nieto, F., Arfè, G., Boni, M. & Mondillo, N. Zn-clay minerals in the Skorpion Zn nonsulfide deposit (Namibia): Identification and genetic clues revealed by HRTEM and AEM study. *Applied Clay Science* **150**, 309–322 (2017).
119. Chassé, M., Griffin, W. L., O'Reilly, S. Y. & Calas, G. Australian laterites reveal mechanisms governing scandium dynamics in the critical zone. *Geochimica et Cosmochimica Acta* **260**, 292–310 (2019).
120. Stucki, J. W. Chapter 11 - Properties and Behaviour of Iron in Clay Minerals. *Handbook of Clay Science* **5**, 559–611 (2013).
121. Huang, J. *et al.* Fe (II) Redox Chemistry in the Environment. (2021).

122. Chakraborty, S. *et al.* U(VI) Sorption and Reduction by Fe(II) Sorbed on Montmorillonite. *Environmental Science & Technology* **44**, 3779–3785 (2010).
123. Liger, E., Charlet, L. & Van Cappellen, P. Surface catalysis of uranium (VI) reduction by iron(II). *Geochimica Cosmochimica Acta* **63**, 2939–2955 (1999).
124. Brookshaw, D. R. *et al.* Redox interactions of Tc (VII), U (VI), and Np (V) with microbially reduced biotite and chlorite. *Environmental science & technology* **49**, 13139–13148 (2015).
125. Begg, J. D., Edelman, C., Zavarin, M. & Kersting, A. B. Sorption kinetics of plutonium (V)/(VI) to three montmorillonite clays. **96**, 131–137 (2018).
126. Hixon, A. E. & Powell, B. A. Plutonium environmental chemistry: mechanisms for the surface-mediated reduction of Pu (v/vi). **20**, 1306–1322 (2018).
127. Charlet, L. *et al.* Electron transfer at the mineral/water interface: Selenium reduction by ferrous iron sorbed on clay. *Geochimica et Cosmochimica Acta* **71**, 5731–5749 (2007).
128. Ilgen, A. G., Kruichak, J. N., Artyushkova, K., Newville, M. G. & Sun, C. Redox transformations of As and Se at the surfaces of natural and synthetic ferric nontronites: role of structural and adsorbed Fe (II). *Environmental science & technology* **51**, 11105–11114 (2017).
129. Bishop, M. E., Dong, H., Kukkadapu, R. K., Liu, C. & Edelmann, R. E. Bioreduction of Fe-bearing clay minerals and their reactivity toward pertechnetate (Tc-99). *Geochimica et Cosmochimica Acta* **75**, 5229–5246 (2011).
130. Jaisi, D. P. *et al.* Reduction and long-term immobilization of technetium by Fe (II) associated with clay mineral nontronite. *Chemical Geology* **264**, 127–138 (2009).
131. Qafoku, O. *et al.* Tc (VII) and Cr (VI) interaction with naturally reduced ferruginous smectite from a redox transition zone. *Environmental science & technology* **51**, 9042–9052 (2017).
132. Brigatti, M. F. *et al.* Reduction and sorption of chromium by Fe(II)-bearing phyllosilicates: chemical treatments and X-ray absorption spectroscopy (XAS) studies. *Clays and Clay Minerals* **48**, 272–281 (2000).
133. Joe-Wong, C., Brown Jr, G. E. & Maher, K. Kinetics and products of chromium (VI) reduction by iron (II/III)-bearing clay minerals. *Environmental science & technology* **51**, 9817–9825 (2017).
134. Liao, W. *et al.* Effect of coexisting Fe (III)(oxyhydr) oxides on Cr (VI) reduction by Fe (II)-bearing clay minerals. *Environmental science & technology* **53**, 13767–13775 (2019).
135. Bishop, M. E., Glasser, P., Dong, H., Arey, B. & Kovarik, L. Reduction and immobilization of hexavalent chromium by microbially reduced Fe-bearing clay minerals. *Geochimica et Cosmochimica Acta* **133**, 186–203 (2014).
136. Scheinost, A. C. *et al.* X-ray absorption and photoelectron spectroscopy investigation of selenite reduction by Fe-II-bearing minerals. *Journal of Contaminant Hydrology* **102**, 228–245 (2008).
137. Ilgen, A. G., Foster, A. L. & Trainor, T. P. Role of structural Fe in nontronite NAu-1 and dissolved Fe (II) in redox transformations of arsenic and antimony. *Geochimica et Cosmochimica Acta* **94**, 128–145 (2012).
138. Cheng, J. & Sprik, M. Alignment of electronic energy levels at electrochemical interfaces. *Physical Chemistry Chemical Physics* **14**, 11245–11267 (2012).
139. Blumberger, J. Recent advances in the theory and molecular simulation of biological electron transfer reactions. *Chemical reviews* **115**, 11191–11238 (2015).

140. Cheng, J., Liu, X., Kattirtzi, J. A., VandeVondele, J. & Sprik, M. Aligning Electronic and Protonic Energy Levels of Proton-Coupled Electron Transfer in Water Oxidation on Aqueous TiO₂. *Angewandte Chemie* **126**, 12242–12246 (2014).
141. Anisimov, V. I., Zaanen, J. & Andersen, O. K. Band theory and Mott insulators: Hubbard U instead of Stoner I. *Physical Review B* **44**, 943 (1991).
142. Behler, J., Delley, B., Reuter, K. & Scheffler, M. Nonadiabatic potential-energy surfaces by constrained density-functional theory. *Physical Review B* **75**, 115409 (2007).
143. Alexandrov, V. & Rosso, K. M. Insights into the mechanism of Fe (II) adsorption and oxidation at Fe–Clay mineral surfaces from first-principles calculations. *The Journal of Physical Chemistry C* **117**, 22880–22886 (2013).
144. Liu, X., Cheng, J. & Sprik, M. Aqueous transition-metal cations as impurities in a wide gap oxide: The Cu²⁺/Cu⁺ and Ag²⁺/Ag⁺ redox couples revisited. *The Journal of Physical Chemistry B* **119**, 1152–1163 (2015).
145. Cheng, J. & VandeVondele, J. Calculation of electrochemical energy levels in water using the random phase approximation and a double hybrid functional. *Physical review letters* **116**, 086402 (2016).
146. Cheng, J., Liu, X., VandeVondele, J., Sulpizi, M. & Sprik, M. Redox potentials and acidity constants from density functional theory based molecular dynamics. *Accounts of chemical research* **47**, 3522–3529 (2014).
147. Ferrage, E. *et al.* Hydration properties and interlayer organization of water and ions in synthetic Na-smectite with tetrahedral layer charge. Part 2. Toward a precise coupling between molecular simulations and diffraction data. *The Journal of Physical Chemistry C* **115**, 1867–1881 (2011).
148. Tambach, T. J., Hensen, E. J. M. & Smit, B. Molecular simulations of swelling clay minerals. *The Journal of Physical Chemistry B* **108**, 7586–7596 (2004).
149. Le Crom, S., Tournassat, C., Robinet, J.-C. & Marry, V. Influence of Water Saturation Level on Electrical Double Layer Properties in a Clay Mineral Mesopore: A Molecular Dynamics Study. *The Journal of Physical Chemistry C* (2022).
150. Savoye, S., Beaucaire, C., Fayette, A., Herbette, M. & Coelho, D. Mobility of cesium through the callovo-oxfordian claystones under partially saturated conditions. *Environmental Science & Technology* **46**, 2633–2641 (2012).
151. Huang, B. *et al.* Effects of soil particle size on the adsorption, distribution, and migration behaviors of heavy metal (loid) s in soil: a review. *Environmental Science: Processes & Impacts* **22**, 1596–1615 (2020).
152. Kleber, M. *et al.* Mineral–organic associations: formation, properties, and relevance in soil environments. *Advances in agronomy* **130**, 1–140 (2015).
153. Lagaly, G., Ogawa, M. & Dékény, I. Chapter 10.3 - Clay Mineral - Organic Interactions. *Handbook of Clay Science* **5**, 435–505 (2013).
154. Kleber, M. *et al.* Dynamic interactions at the mineral–organic matter interface. *Nature Reviews Earth & Environment* **2**, 402–421 (2021).
155. Sutton, R. & Sposito, G. Molecular structure in soil humic substances: the new view. *Environmental science & technology* **39**, 9009–9015 (2005).
156. Piccolo, A. The supramolecular structure of humic substances. *Soil science* **166**, 810–832 (2001).
157. Schnitzer, M. A lifetime perspective on the chemistry of soil organic matter. *Advances in agronomy* **68**, 1–58 (1999).

158. Stevenson, F. J. *Humus chemistry: genesis, composition, reactions*. (John Wiley & Sons: 1994).
159. Colombo, C. *et al.* Spontaneous aggregation of humic acid observed with AFM at different pH. *Chemosphere* **138**, 821–828 (2015).
160. Kelleher, B. P. & Simpson, A. J. Humic substances in soils: are they really chemically distinct? *Environmental science & technology* **40**, 4605–4611 (2006).
161. Petrov, D., Tunega, D., Gerzabek, M. H. & Oostenbrink, C. Molecular dynamics simulations of the standard leonardite humic acid: Microscopic analysis of the structure and dynamics. *Environmental Science & Technology* **51**, 5414–5424 (2017).
162. Zhang, Y., Liu, X., Zhang, C. & Lu, X. A combined first principles and classical molecular dynamics study of clay-soil organic matters (SOMs) interactions. *Geochimica et Cosmochimica Acta* **291**, 110–125 (2020).
163. Willemsen, J. A., Myneni, S. C. & Bourg, I. C. Molecular dynamics simulations of the adsorption of phthalate esters on smectite clay surfaces. *The Journal of Physical Chemistry C* **123**, 13624–13636 (2019).
164. Tournassat, C., Steefel, C., Bourg, I. & Bergaya, F. *Natural and engineered clay barriers*. **6**, (Elsevier: 2015).
165. Gates, W. P., Bouazza, A. & Churchman, G. J. Bentonite clay keeps pollutants at bay. *Elements* **5**, 105–110 (2009).
166. Otunola, B. O. & Ololade, O. O. A review on the application of clay minerals as heavy metal adsorbents for remediation purposes. *Environmental Technology & Innovation* **18**, 100692 (2020).
167. Delage, P., Cui, Y.-J. & Tang, A. M. Clays in radioactive waste disposal. *Journal of Rock Mechanics and Geotechnical Engineering* **2**, 111–123 (2010).
168. Mukherjee, S. Uses of clays in waste managements: toxic and non-toxic. *The Science of Clays* 309–325 (2013).
169. Sellin, P. & Leupin, O. X. The use of clay as an engineered barrier in radioactive-waste management—a review. *Clays and Clay Minerals* **61**, 477–498 (2013).
170. Wypych, F., Bergaya, F. & Schoonheydt, R. A. From polymers to clay polymer nanocomposites. *Developments in clay science* **9**, 331–359 (2018).
171. Bergaya, F. & Lagaly, G. Chapter 10.0 - Introduction on Modified Clays and Clay Minerals. *Handbook of Clay Science* **5**, 383 – (2013).
172. Vicente, M. A., Gil, A. & Bergaya, F. Chapter 10.5 - Pillared Clays and Clay Minerals. *Handbook of Clay Science* **5**, 523–557 (2013).
173. Dutta, D. K. Clay mineral catalysts. *Developments in Clay Science* **9**, 289–329 (2018).
174. Bhowmick, S. *et al.* Montmorillonite-supported nanoscale zero-valent iron for removal of arsenic from aqueous solution: Kinetics and mechanism. *Chemical Engineering Journal* **243**, 14–23 (2014).
175. Han, H. *et al.* A critical review of clay-based composites with enhanced adsorption performance for metal and organic pollutants. *Journal of hazardous materials* **369**, 780–796 (2019).
176. Yadav, V. B., Gadi, R. & Kalra, S. Clay based nanocomposites for removal of heavy metals from water: A review. **232**, 803–817 (2019).
177. Zhang, T. *et al.* Removal of heavy metals and dyes by clay-based adsorbents: From natural clays to 1D and 2D nano-composites. *Chemical Engineering Journal* 127574 (2020).

178. Buruga, K. *et al.* A review on functional polymer-clay based nanocomposite membranes for treatment of water. *Journal of hazardous materials* **379**, 120584 (2019).
179. Jlassi, K., Chehimi, M. M. & Thomas, S. *Clay-polymer nanocomposites*. (Elsevier: 2017).
180. Payne, T. E. *et al.* Guidelines for thermodynamic sorption modelling in the context of radioactive waste disposal. *Environmental modelling & software* **42**, 143–156 (2013).
181. Caporale, A. G. & Violante, A. Chemical processes affecting the mobility of heavy metals and metalloids in soil environments. *Current Pollution Reports* **2**, 15–27 (2016).
182. Manceau, A. *et al.* Quantitative Zn speciation in smelter-contaminated soils by EXAFS spectroscopy. *American Journal of Science* **300**, 289–343 (2000).
183. Appelo, C. A. J., Vinsot, A., Mettler, S. & Wechner, S. Obtaining the porewater composition of a clay rock by modeling the in- and out-diffusion of anions and cations from an in-situ experiment. *Journal of Contaminant Hydrology* **101**, 67–76 (2008).
184. Appelo, C. A. J. & Wersin, P. Multicomponent diffusion modeling in clay systems with application to the diffusion of tritium, iodide, and sodium in Opalinus clay. *Environmental Science & Technology* **41**, 5002–5007 (2007).
185. Soler, J. M., Steefel, C. I., Gimmi, T., Leupin, O. X. & Cloet, V. Modeling the ionic strength effect on diffusion in clay. The DR-A experiment at Mont Terri. *ACS Earth and Space Chemistry* **3**, 442–451 (2019).
186. Gimmi, T. & Kosakowski, G. How mobile are sorbed cations in clays and clay rocks? *Environmental Science & Technology* **45**, 1443–1449 (2011).
187. Glaus, M. *et al.* Cation diffusion in the electrical double layer enhances the mass transfer rates for Sr²⁺, Co²⁺ and Zn²⁺ in compacted illite. *Geochimica et Cosmochimica Acta* **165**, 376–388 (2015).
188. Glaus, M., Frick, S. & Van Loon, L. A coherent approach for cation surface diffusion in clay minerals and cation sorption models: Diffusion of Cs⁺ and Eu³⁺ in compacted illite as case examples. *Geochimica et Cosmochimica Acta* **274**, 79–96 (2020).
189. Borst, A. M. *et al.* Adsorption of rare earth elements in regolith-hosted clay deposits. *Nature communications* **11**, 1–15 (2020).
190. Chi, R., Tian, J. & others *Weathered crust elution-deposited rare earth ores*. (Nova Science Publishers: 2008).
191. Li, Y. H. M., Zhao, W. W. & Zhou, M.-F. Nature of parent rocks, mineralization styles and ore genesis of regolith-hosted REE deposits in South China: an integrated genetic model. *Journal of Asian Earth Sciences* **148**, 65–95 (2017).
192. Moldoveanu, G. & Papangelakis, V. An overview of rare-earth recovery by ion-exchange leaching from ion-adsorption clays of various origins. *Mineralogical Magazine* **80**, 63–76 (2016).
193. Sanematsu, K., Kon, Y., Imai, A., Watanabe, K. & Watanabe, Y. Geochemical and mineralogical characteristics of ion-adsorption type REE mineralization in Phuket, Thailand. **48**, 437–451 (2013).
194. Li, M. Y. H., Zhou, M.-F. & Williams-Jones, A. E. The genesis of regolith-hosted heavy rare earth element deposits: Insights from the world-class Zudong deposit in Jiangxi Province, South China. *Economic Geology* **114**, 541–568 (2019).
195. Goodenough, K. M., Wall, F. & Merriman, D. The rare earth elements: demand, global resources, and challenges for resourcing future generations. *Natural Resources Research* **27**, 201–216 (2018).
196. Jordens, A., Cheng, Y. P. & Waters, K. E. A review of the beneficiation of rare earth element bearing minerals. *Minerals Engineering* **41**, 97–114 (2013).

- 1196 197. Berger, A., Janots, E., Gnos, E., Frei, R. & Bernier, F. Rare earth element mineralogy and
1197 geochemistry in a laterite profile from Madagascar. *Applied geochemistry* **41**, 218–228
1198 (2014).
- 1199 198. Bern, C. R., Yesavage, T. & Foley, N. K. Ion-adsorption REEs in regolith of the Liberty Hill
1200 pluton, South Carolina, USA: an effect of hydrothermal alteration. *Journal of*
1201 *Geochemical Exploration* **172**, 29–40 (2017).
- 1202 199. Sanematsu, K. & Watanabe, Y. Characteristics and Genesis of Ion Adsorption-Type Rare
1203 Earth Element Deposits. *Rare Earth and Critical Elements in Ore Deposits* (2016).
- 1204 200. Yamaguchi, A., Honda, T., Tanaka, M., Tanaka, K. & Takahashi, Y. Discovery of ion-
1205 adsorption type deposits of rare earth elements (REE) in Southwest Japan with
1206 speciation of REE by extended X-ray absorption fine structure spectroscopy.
1207 *Geochemical Journal* **52**, 415–425 (2018).
- 1208 201. Braun, J.-J. *et al.* Cerium anomalies in lateritic profiles. *Geochimica et Cosmochimica*
1209 *Acta* **54**, 781–795 (1990).
- 1210 202. Takahashi, Y., Shimizu, H., Usui, A., Kagi, H. & Nomura, M. Direct observation of
1211 tetravalent cerium in ferromanganese nodules and crusts by X-ray-absorption near-
1212 edge structure (XANES). *Geochimica et Cosmochimica Acta* **64**, 2929–2935 (2000).
- 1213 203. Moldoveanu, G. A. & Papangelakis, V. G. Recovery of rare earth elements adsorbed on
1214 clay minerals: I. Desorption mechanism. *Hydrometallurgy* **117**, 71–78 (2012).
- 1215 204. Jones, D. J., Rozière, J., Olivera-Pastor, P., Rodríguez-Castellón, E. & Jimenez-López, A.
1216 Local environment of intercalated lanthanide ions in vermiculite. *Journal of the*
1217 *Chemical Society, Faraday Transactions* **87**, 3077–3081 (1991).
- 1218 205. Takahashi, Y., Kimura, T., Kato, Y., Minai, Y. & Tominaga, T. Characterization of Eu (III)
1219 species sorbed on silica and montmorillonite by laser-induced fluorescence
1220 spectroscopy. *Radiochimica Acta* **82**, 227–232 (1998).
- 1221 206. Stumpf, T., Bauer, A., Coppin, F., Fanghänel, T. & Kim, J.-I. Inner-sphere, outer-sphere
1222 and ternary surface complexes: a TRLFS study of the sorption process of Eu (III) onto
1223 smectite and kaolinite. *Radiochimica Acta* **90**, 345–349 (2002).
- 1224 207. Mukai, H., Kon, Y., Sanematsu, K., Takahashi, Y. & Ito, M. Microscopic analyses of
1225 weathered granite in ion-adsorption rare earth deposit of Jianxi Province, China.
1226 *Scientific reports* **10**, 1–11 (2020).
- 1227 208. Velde, B. B. & Meunier, A. *The origin of clay minerals in soils and weathered rocks.*
1228 (Springer Science & Business Media: 2008).
- 1229 209. Nagasawa, M., Qin, H.-B., Yamaguchi, A. & Takahashi, Y. Local Structure of Rare Earth
1230 Elements (REE) in Marine Ferromanganese Oxides by Extended X-ray Absorption Fine
1231 Structure and Its Comparison with REE in Ion-adsorption Type Deposits. *Chemistry*
1232 *Letters* **49**, 909–911 (2020).
- 1233 210. Ohta, A., Kagi, H., Tsuno, H., Nomura, M. & Kawabe, I. Influence of multi-electron
1234 excitation on EXAFS spectroscopy of trivalent rare-earth ions and elucidation of change
1235 in hydration number through the series. *American Mineralogist* **93**, 1384–1392 (2008).
- 1236 211. Stumpf, S. *et al.* Sorption of Am (III) onto 6-line-ferrihydrite and its alteration products:
1237 Investigations by EXAFS. *Environmental science & technology* **40**, 3522–3528 (2006).
- 1238 212. Ohta, A., Kagi, H., Nomura, M., Tsuno, H. & Kawabe, I. Coordination study of rare earth
1239 elements on Fe oxyhydroxide and Mn dioxides: Part II. Correspondence of structural
1240 change to irregular variations of partitioning coefficients and tetrad effect variations
1241 appearing in interatomic distances. *American Mineralogist* **94**, 476–486 (2009).

213. Kashiwabara, T. *et al.* Synchrotron X-ray spectroscopic perspective on the formation mechanism of REY-rich muds in the Pacific Ocean. *Geochimica et Cosmochimica Acta* **240**, 274–292 (2018).
214. Butt, C. R. & Cluzel, D. Nickel laterite ore deposits: weathered serpentinites. *Elements* **9**, 123–128 (2013).
215. Bergaya, F. & Lagaly, G. Chapter 1 - General Introduction: Clays, Clay Minerals, and Clay Science. *Handbook of Clay Science. Part A. Fundamentals* **5**, 1–19 (2013).
216. Schoonheydt, R. A., Johnston, C. T. & Bergaya, F. Clay minerals and their surfaces. *Developments in Clay Science* **9**, 1–21 (2018).
217. Hohenberg, P. & Kohn, W. Inhomogeneous electron gas. *Physical review* **136**, B864 (1964).
218. Kohn, W. & Sham, L. J. Self-consistent equations including exchange and correlation effects. *Physical review* **140**, A1133 (1965).
219. Marx, D. & Hutter, J. *Ab initio molecular dynamics: basic theory and advanced methods*. (Cambridge University Press: 2009).
220. Frenkel, D. & Smit, B. *Understanding molecular simulation: from algorithms to applications*. (Academic Press: 2002).
221. Liu, X., Tournassat, C. & Steefel, C. I. Preface to multiscale simulation in geochemistry. **291**, 1–4 (2020).
222. Sposito, G. *The surface chemistry of natural particles*. 242 (Oxford University Press: New York, 2004).
223. Steefel, C. I. *et al.* Reactive transport codes for subsurface environmental simulation. *Computational Geosciences* **19**, 445–478 (2015).
224. Steefel, C. I. Reactive transport at the crossroads. *Reviews in Mineralogy & Geochemistry* **85**, 1–26 (2019).

Acknowledgements

XL was supported by the National Natural Science Foundation of China (Nos. 42125202 and 41872041). CT, SG and AMF acknowledge funding from the EC Horizon 2020 project EURAD under Grant Agreement 847593 (WP FUTURE). CT research at LBNL was supported by the U.S. Department of Energy, Office of Science, Office of Basic Energy Sciences, Chemical Sciences, Geosciences, and Biosciences Division, through its Geoscience program at LBNL under Contract DE-AC02-05CH11231. CT acknowledges a grant overseen by the French National Research Agency (ANR) as part of the “Investissements d’Avenir” Programme LabEx VOLTAIRE, 10-LABX-0100 at ISTO. S.G. acknowledges partial funding by an in-house BRGM grant.

Author contributions

XL and CT were responsible for the design and compilation of the article. All authors contributed to the writing and editing.

Competing interests

The authors declare no competing interests.

Peer review information

Nature Reviews Earth & Environment thanks J. Kubicki, B. Sarkar, and the other, anonymous, reviewer(s) for their contribution to the peer review of this work.

Publisher's note

Springer Nature remains neutral with regard to jurisdictional claims in published maps and institutional affiliations.

Key points:

- Clay minerals have a diverse array of chemical structures and layer types that lead to a range of metal ion retention mechanisms in Earth's critical zone. The metal retention capabilities of clay minerals can concentrate rare earth elements (REEs) in ion adsorption type deposits and can also be exploited for metallic industrial waste disposal.
- Basic metal ion-clay mineral interaction mechanisms include cation exchange, surface complexation, ligand exchange, structural incorporation, surface precipitation (with or without epitaxial growth of neoformed minerals), and precipitation induced by surface redox reactions.
- Such diversity of retention mechanisms originates from the distinct structures and properties of basal and edge surfaces. Cation exchange on basal surfaces occurs mainly through electrostatics while other mechanisms occur through chemical bonding on edge surfaces.
- REEs in ion adsorption type deposits are mainly physically adsorbed on basal surfaces, which are responsible for the high REE extractability (> 50 %) through ion exchange.
- Both cation exchange and surface complexation processes occur during the retardation of metallic pollution plumes in waste management applications (radioactive and conventional industrial wastes as well as landfill leachate).
- Understanding and quantification of the multifaceted and multiscale nature of clay mineral-metal ion interactions necessitates the close combination of experimental and modelling techniques at the molecular-level.

Figures

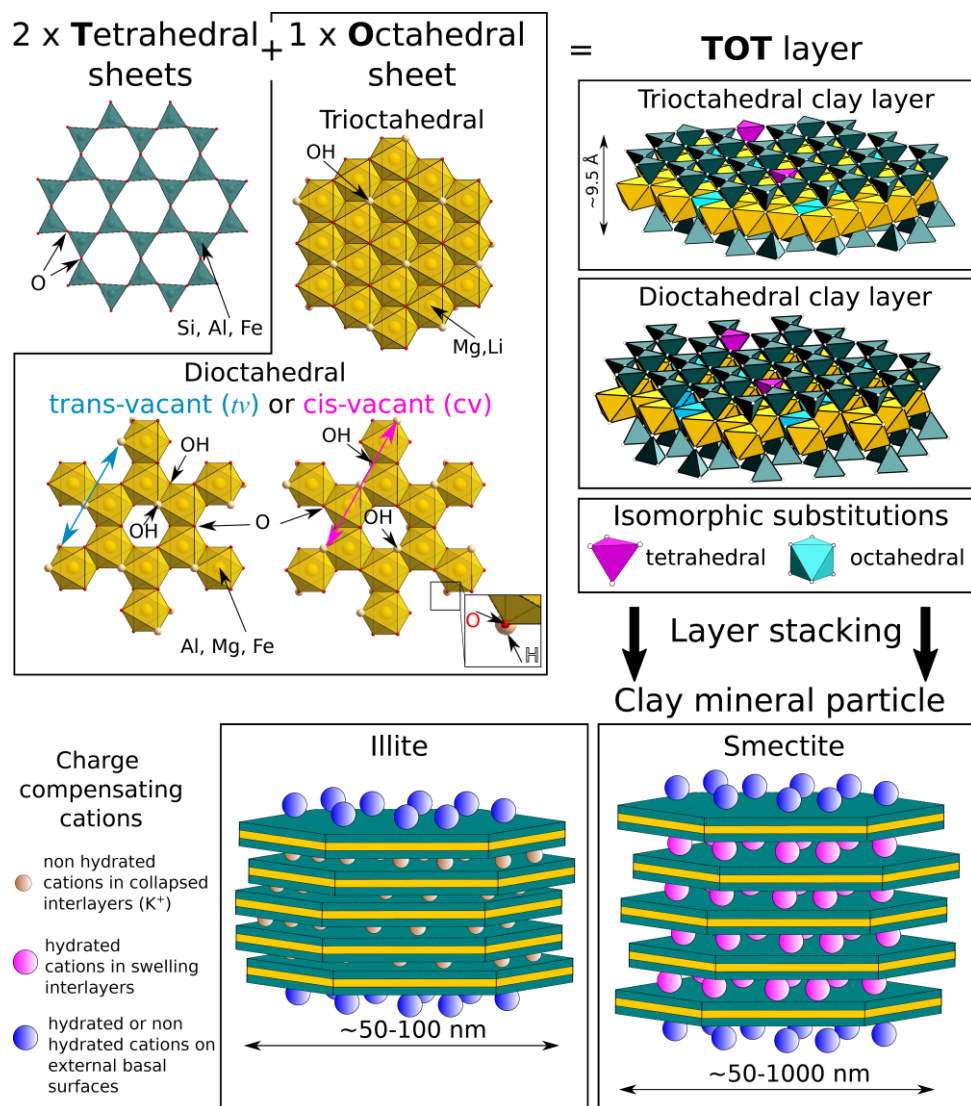


Figure 1. Clay mineral sheet, layer and particle structures. Two tetrahedral sheets sandwiching an octahedral sheet form a tetrahedral-octahedral-tetrahedral (TOT) layer. The thickness of a TOT layer, $\sim 9.5 \text{ \AA}$, corresponds to the distance between two planes of apical oxygen atoms, $\sim 6.6 \text{ \AA}$, plus the ionic radii of two oxygen atoms. Isomorphous substitutions (where one structural cation is replaced for another of similar size, see magenta tetrahedral and cyan octahedral) are responsible for a permanent negative structural layer charge that is compensated by cations present in the interlayer spaces and on external surfaces of clay mineral particles. In water-saturated conditions, charge compensating cations can be hydrated (red and blue cations) or not (yellow cations), depending on the nature of the cation, the type of layer isomorphous substitutions, the layer charge, and the type of neighbouring surfaces (interlayer versus external). Layer structure and negative charge are responsible for the high metal cation retention capability of clay minerals.

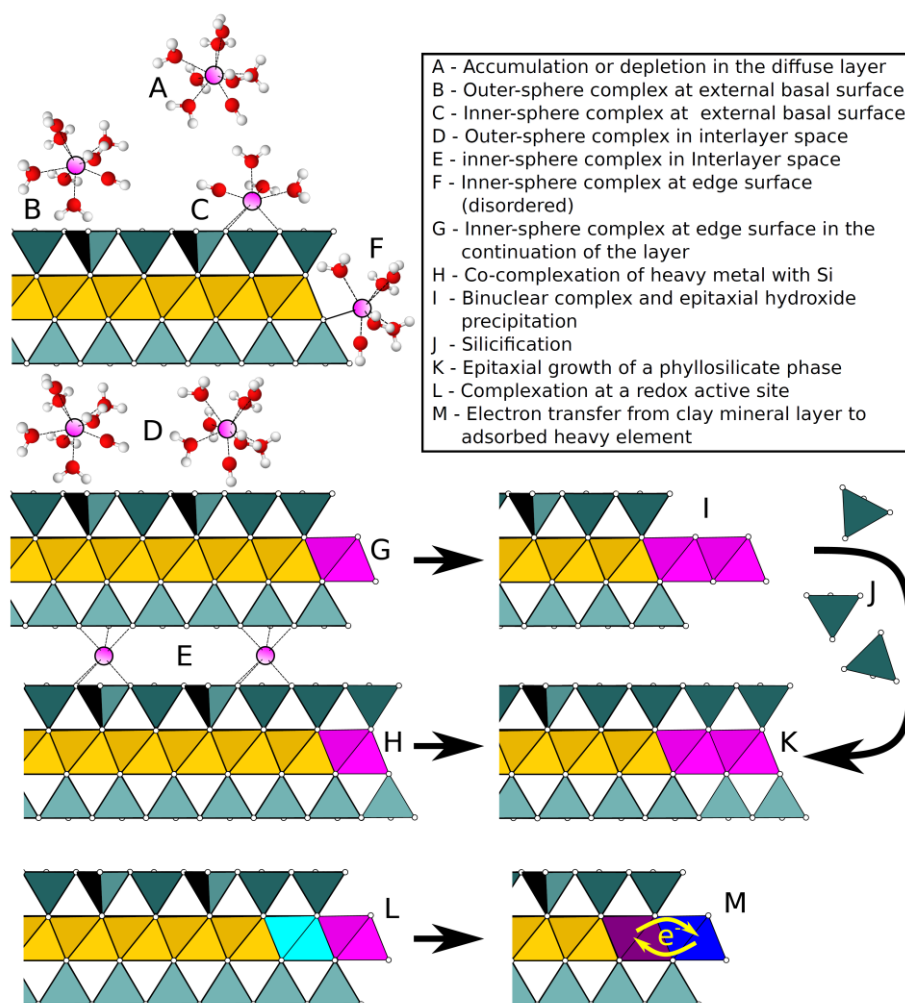


Figure 2. **Interaction mechanisms of metal ions with clay minerals.** Clay layers are made of octahedral (orange) and tetrahedral (blue) sheets, depicted along the stacking direction. Adsorbed metal ions are shown in purple, and water molecules in red and white. a| Metal ions (purple) in complexes with water molecules (red-white) can be adsorbed onto external basal surfaces or accumulate in diffuse layers. The transitions from panels b to d highlight the continuum from adsorption on edge surfaces to clay mineral nucleation and growth. b| outer-sphere complexes can be adsorbed in the interlayer space. Inner-sphere complexes can attach onto the edge of the octahedral layer, or c| in the interlayer space. If complexation of the edge surface occurs at the same time as silicification, the clay mineral undergoes epitaxial growth. d| A cation adsorbed by complexation at an active redox site on an edge surface can undergo electron transfer with the clay mineral layer, which in turn changes the redox state of both the octahedral sheet and adsorbed metal ions (blue-purple colour change). The duality of surface types (basal vs. edge) and the redox reactivity of the inner atoms in the layer are responsible for multiple modes of interactions with metal cations.

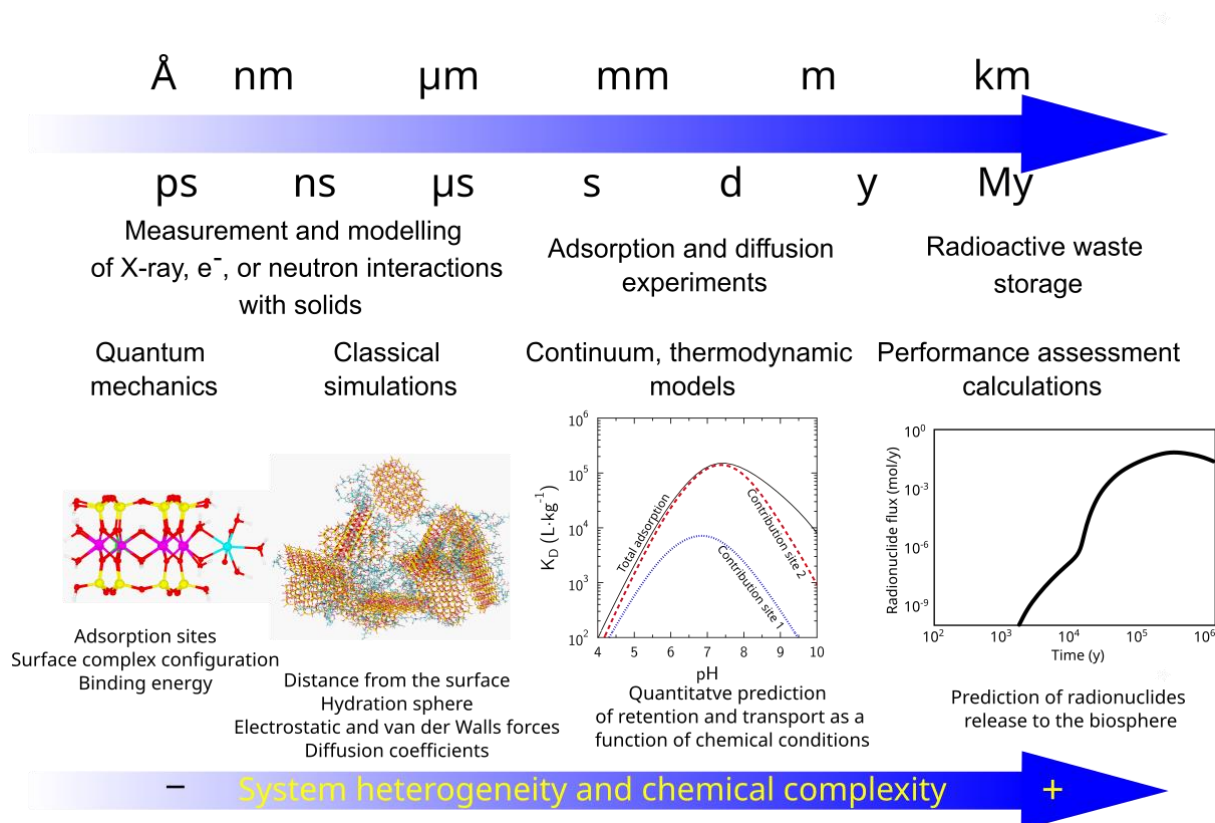


Figure 3. **Upscaling of information in modeling of radionuclide storage.** a| Quantum mechanical simulation of a metal ion complexed on clay mineral surface. b| Classical simulation of metal ions at a clay mineral-aqueous solution interface. c| An example of a surface complexation model for metal ion adsorption on clay mineral surfaces using a two-site model. Information about binding energy and the nature of adsorption sites can be constrained by molecular level studies. d| generic example of a simulation of radionuclide flux at the outlet of a radioactive waste storage site over 1000-100,000 year time scales. Retention and diffusion parameters used in these simulations are usually obtained in laboratory experiments that last from days to years. Using these parameters to make upscaled predictions to million year time scales must be justified by process understanding and quantification. Effective upscaling of molecular-level information from measurements and simulations enables practical applications in macroscopic studies.

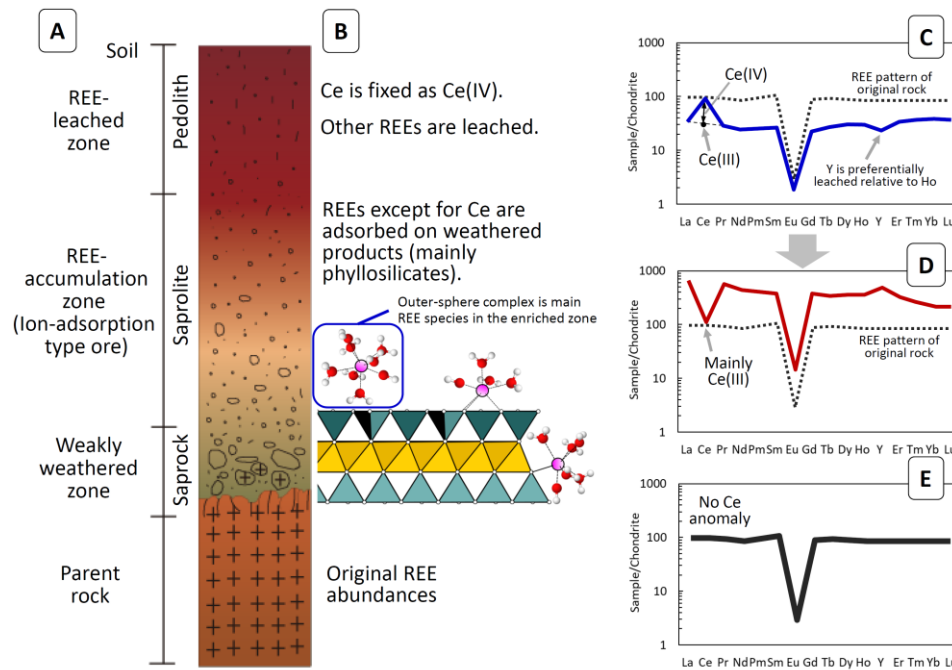


Figure 4. Ion-adsorption type rare earth element (REE) deposits. a | Typical vertical profile of weathered zone hosting ion-adsorption deposit (IAD). Granite is a typical parent rock for IADs. **b** | Rare earth elements, excluding Ce, are leached from the top layer in the profile (the pedolith). REE accumulation occurs in saprolite deposits, below the pedolith but above the weathered parent rock. Adsorption of REEs in the accumulation zone mainly occurs as outer-sphere complexes on external basal clay layers. **c** | the REE-leached zone is characterized by a positive cerium (Ce) anomaly and relatively low REE abundances. Y is preferentially leached relative to Ho. **d** | the REE-accumulation zone is characterized by a negative Ce anomaly and enrichment of the other REEs. Y is enriched relative to Ho. **e** | the weakly weathered zone has a similar REE pattern to the parent rock, but does not have the Ce anomaly. Adsorption on clay minerals as outer-sphere complex is responsible for the enrichment and high extraction rate of REEs in IAD.

Boxes

Box 1. Clay mineral structures and surfaces

Clay minerals are phyllosilicates. They are made up of stacked layers consisting of an assemblage of sheets. Chemical composition, spatial arrangement of sheets, and layer stacking mode are the main criteria that identify clay mineral family members²¹⁵.

Layers of dioctahedral smectite and illite, two groups of clay minerals of interest for their metal ions retention properties, are made of two tetrahedral sheets sandwiching an octahedral sheet, forming so-called 2:1 layers (Figure 1).

Tetrahedral and octahedral sheets of smectite and illite contain mostly Si and Al (or Fe) atoms. A range of other minor elements are incorporated through isomorphic substitutions, which create a local charge imbalance if the substituted element does not bear the same formal charge as the incorporated element (for example, Mg^{2+} for Al^{3+}). This local charge is not compensated for in the layer structure, which creates a permanent negative structural charge in the clay layer. This negative charge is compensated by the positive charge of cations in the interlayer space and on external surfaces.

Interlayer spaces can be hydrated and accessible to aqueous species as in the case of smectite, or collapsed and mostly inaccessible to water and aqueous species as in the case of illite, in which adjacent tetrahedral sheets are bonded by non-hydrated K^+ ions (Figure 1). Na^+ , K^+ , Ca^{2+} , Mg^{2+} are the most common charge compensating cations, but they can be exchanged easily on external and hydrated interlayer surfaces by other metal cations⁶⁸. Differences in hydration properties of interlayer cations results in the common phenomenon of clay mineral swelling, which corresponds to changes of interlayer spacing as a function of the nature of interlayer cations and water chemical potential²¹⁶.

Crystal faces of clay minerals can be grouped into basal and edge surfaces, which are parallel and perpendicular to the basal plane respectively⁶⁸. Smectite and illite layers thickness is approximately 1 nm, while their lateral dimensions range from 50 nm to 1 μm (Figure 1). These dimensions result in very large specific surface areas, up to 800 $\text{m}^2 \text{g}^{-1}$ for smectites. The vast majority of the surface area is born by the basal surfaces, while edge surface area account for only 5 to 30 $\text{m}^2 \text{g}^{-1}$.

Atoms present at basal surfaces are fully coordinated and form a siloxane terminated surface, while oxygen atoms present at edge surfaces have fewer metal neighbours than in bulk (Figure 1). Edge surfaces are covered by chemically adsorbed water, forming amphoteric charged surface hydroxyl groups ($>\text{OH}$ groups, where the $>$ sign is indicative of a surface coordination), having contrasted acidity constants (pK_a) as a function of coordination, surface crystallographic orientation and nature of the central metal bonded to the $>\text{OH}$ group⁸⁸. Consequently, edge surface chemical properties are strongly pH-dependent, by contrast, basal surface properties are little or not.

Box 2. Quantification of metal ion immobilisation

Macroscopic quantification of metal ion retention on a given mass of clay minerals (m_{clay} in kg) can be obtained from experimental adsorption isotherms (see figure). The concentration of an adsorbed element (C_{ads} in $\text{mol kg}^{-1}_{\text{clay}}$) can be quantified by the difference between a total concentration added in the system (C_{tot} in mol L^{-1}) and an aqueous concentration measured at steady-state, which is assumed to be representative of thermodynamic equilibrium (C_{eq} in mol L^{-1}).

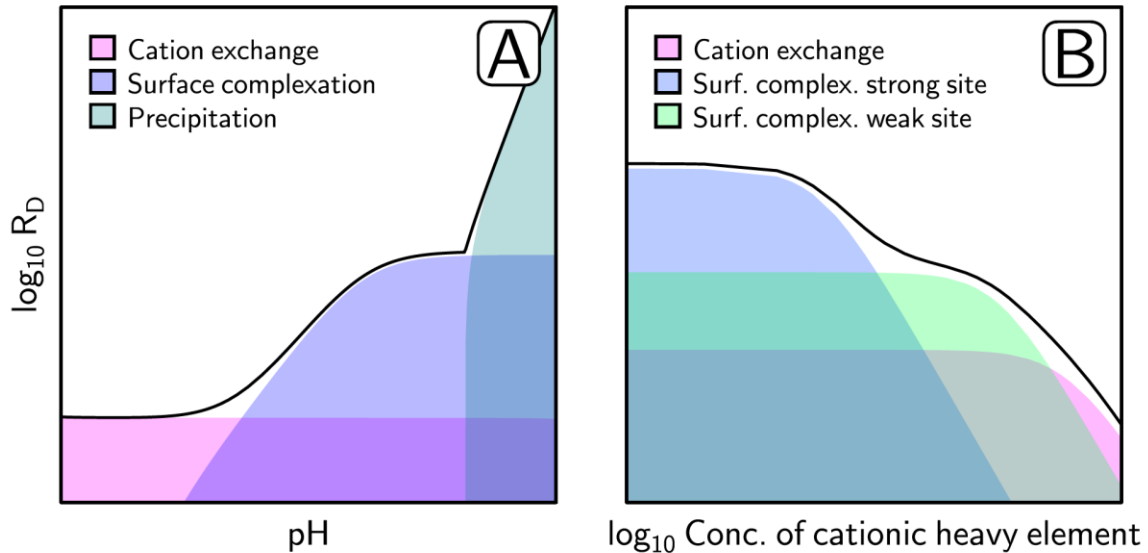
Retention is usually quantified as a percentage of total added concentration, or as a distribution coefficient R_D , or K_D (in L kg^{-1}), which quantify the partitioning of the metal ions between the solution and the surface:

$$C_{\text{ads}} = \frac{C_{\text{tot}} - C_{\text{eq}}}{m_{\text{clay}}} V_{\text{sol}} \quad 1$$

$$R_D \text{ or } K_D = \frac{C_{\text{ads}}}{C_{\text{eq}}} \quad 2$$

where V_{sol} is the volume of solution (in L).

The R_D value does not give any insight into the physical and chemical processes responsible for the observed retention (such as adsorption, incorporation, and precipitation). However, in a first approach, the shape of the adsorption isotherms plotted as a function of pH and metal ion concentration (see figure), allows the difference between major adsorption sites and other retention mechanisms to be determined.



The figure shows: **a**| retention processes shown as a function of pH and constant metal cations concentration, and **b**| as a function of metal cations concentration and fixed pH. Superposition of coloured areas is indicative of a mixed contribution of several mechanisms to the overall retention.

Box 3. Predictive approaches at different scales

Quantum mechanics simulation

Density functional theory (DFT)^{217,218} has been the workhorse of quantum mechanics calculation. By transforming the 3N-dimensional Schrodinger equation to 3-dimensional Kohn-Sham equation, DFT makes it affordable to calculate energy and atomic forces of realistic systems. First principles molecular dynamics (FPMD)²¹⁹, a combination of DFT and molecular dynamics (MD), generates dynamical trajectories at limited temperatures and is thus able to explore the properties of aqueous and interfacial systems. FPMD can calculate free energy by integrating with enhanced sampling techniques (such as the method of constraint, metadynamics). However, the expensive computational costs badly limits the system size and time FPMD can access: for current supercomputing architecture the typical length and time scales are only ~10 angstroms and ~10 picoseconds.

Classical simulation

Classical simulation calculates energy and forces based on a force field that is a set of parameters describing atomic interactions²²⁰. Classical MD produces dynamical trajectories by using the forces calculated from a force field. The length and timescale of classical simulation can reach second and micrometer.

Multiscale simulation

Classical mechanical simulation and thermodynamic models are necessary to build direct link to macroscopic experiments. These models are usually based on a set of empirical/fitted parameters. Multiscale simulation plays the role of a bridge by translating the information generated by quantum mechanics into parameters of upscaling modelling, thus overcoming the temporal and spatial limits of quantum mechanics modelling, such as it provides constraints for geochemical modeling and the force field used in classical simulation²²¹.

Geochemical thermodynamic modeling

Surface complexation and cation exchange models apply mass balance, surface charge balance and thermodynamic chemical equilibrium concepts to predict, quantitatively, the partitioning of chemical species between an aqueous solution and mineral surfaces²²². Surface complexation and cation exchange models can be coupled to fluid transport models at large scale (aquifers, rivers, water catchment) to build defensible predictions in the environmental sciences^{223,224}. Since the ~2000s, model parameters have been obtained from fitting macroscopic adsorption, while microscopic and spectroscopic observations helped constraining the main mechanisms responsible for the observed metal ions retention. Since the ~2010s, advances in molecular level modelling and multiscale simulations provide new

possibilities to reduce the number of empirical fitting parameters in surface complexation and cation exchange models.

Glossary terms:

Metal ions: metal cation (M) in aqueous solution with the chemical formula $[M(H_2O)_n]^{z+}$, metal ions include rare earth elements (REEs), actinides, transition metals, and alkaline and alkaline-earth metals.

Clay mineral: signifies a class of hydrated phyllosilicates making up the fine-grained fraction of rocks, sediments, and soils, which this Review is focused on.

Clay-rich materials refers to materials containing clay minerals, such as sediments, soils and weathered rocks, and with physical and chemical properties dominated by their clay mineral fraction.

Earth's Critical zone: The oxygenated and hydrated layer at Earth's surface and shallow subsurface, spanning from the tops of tree canopies to the bottom of groundwater.

Complex: a compound consisting of a central atom or ion that is bonded to other atoms or ions, which are called ligands.

Ligand exchange: A type of reaction in which a ligand of a complex is replaced by a different ligand.

Tetrahedral sheet: A 2-dimensional sheet formed by tetrahedral units, each consisting of a metal cation coordinated by four oxygen atoms and linked to three neighbouring tetrahedra by shared oxygen.

Octahedral sheet: A 2-dimensional sheet formed by octahedral units, each consisting of a metal cation coordinated by six oxygen atoms, linked to six neighbouring octahedra by shared edges.

Diocahedral: A common type of octahedral sheet where most of the metal cations are of +3 valence, two-thirds of the octahedra are occupied while the other third is vacant.

2:1-type clay mineral: clay mineral which has a structural layer made of one octahedral sheet sandwiched by two tetrahedral sheets.

Smectite: A group of 2:1-type clay minerals with expandable interlayer space

Illite: A group of 2:1-type clay minerals with non-expandable interlayer space.

Inner-sphere complex: where the cation is adsorbed on a clay layer with direct chemical contact to the mineral layer surface.

Outer-sphere complex: where the cation is adsorbed on a clay layer surface, but is separated by one or more water molecules.

Epitaxial nucleation: formation of a crystalline nucleus on a substrate, where the new crystalline layers form with one or more well-defined orientations fixed by that of the substrate lattice.

Neutron diffraction: an experimental technique used to probe the crystallographic properties of materials, including the position of hydrogen atoms, notably by taking advantage of the contrasting interactions of neutrons with hydrogen and deuterium.

Synchrotron X-ray reflectivity (XRR): an experimental technique used to study the detailed surface properties of solids, based on the analysis of X-rays reflected by a surface.

X-ray absorption spectroscopy (XAS): an experimental technique used to study oxidation state and local environment of an atom in a sample, based on analysis of variations in X-ray absorption over a range of photon energies.

Website summary:

Clay minerals can retain metal ions, concentrate rare earth elements and be exploited for industrial waste disposal. This Review discusses the molecular-level mechanisms of metal ion retention in clay minerals and their importance for environmental and industrial applications.

